THEORETICAL AND EXPERIMENTAL INVESTIGATION OF PUNCHING PROCESS OF DP800 AUTOMOTIVE STEEL SHEET WITH DIFFERENT PUNCH TIPS

ABDULSALAM ABUBAKER ELAMEN SAIER

2020
MASTER THESIS
MECHANICAL ENGINEERING

Thesis Advisor
Prof. Dr. Bilge DEMİR

THEORETICAL AND EXPERIMENTAL INVESTIGATION OF PUNCHING PROCESS OF DP800 AUTOMOTIVE STEEL SHEET WITH DIFFERENT PUNCH TIPS

Abdulsalam Abubaker Elamen SAIER

T.C
Karabük University
Institute of Graduate Programs
Department of Mechanical Engineering
Prepared as
Master Thesis

Thesis Advisor
Prof. Dr. Bilge DEMİR

Karabuk
December 2020

I certify that in my opinion the thesis submitted by Abdulsalam Abubaker Elamen SAIER titled "THEORETICAL AND EXPERIMENTAL INVESTIGATION OF THE PUNCHING PROCESS OF DP800 AUTOMOTIVE SHEET STEEL WITH DIFFERENT PUNCH TIPS" is fully adequate in scope and in quality as a thesis for the degree of Master of Science.

Prof. Dr. Bilge DEMİR ……

Thesis Advisor, Department of Mechanical Engineering

This thesis is accepted by the examining committee with a unanimous vote in the Department of Manufacturing Engineering as a Master of Science thesis. 21/01/2021

Examining Committee Members (Institutions)	Signature
Chairman : Assoc. Prof. Dr. Okan ÜNAL (KBU)	.....
Member : Prof. Dr. Bilge DEMİR (KBU)	.....
Member : Assoc. Prof. Dr. Hakan GÜRÜN (GU)	.....

The degree of Master of Science by the thesis submitted is approved by the Administrative Board of the Institute of Graduate Programs, Karabük University.

Prof. Dr. Hasan SOLMAZ .....

Head of the Institute of Graduate Programs

"I declare that all the information within this thesis has been gathered and presented in accordance with academic regulations and ethical principles and I have according to the requirements of these regulations and principles cited all those which do not originate in this work as well."

Abdulsalam Abubaker Elamen SAIER

ABSTRACT

Master Thesis

THEORETICAL AND EXPERIMENTAL INVESTIGATION OF PUNCHING PROCESS OF DP800 AUTOMOTIVE STEEL SHEET WITH DIFFERENT PUNCH TIPS

Abdulsalam Abubaker Elamen SAIER

Karabük University
Institute of Graduate Programs
Department of Mechanical Engineering

Thesis Advisor:
Prof. Dr. Bilge DEMİR
December 2020, 66 pages

With the increasing awareness of the importance of automobile lightness, the use of AHSS steels with good lightness, strength and ductility combinations in production has also increased. The increasing of the strength of AHSS steels also limits the application of manufacturing processes such as cutting and punching. One of the most used manufacturing methods during automobile manufacturing is punching. Although it is a simple process, its dependence on many parameters makes it difficult to obtain quality outputs due to optimization studies. Punching process of good quality depends on some parameters such as clearance, punch force, punch speed, blank-holder force and punch tip geometry. The punch force is the most complex one of these parameters, as it is linked to many parameters. The most important parameter affecting the cutting force is the punch tip geometry. Although there have been many studies in the literature on the effects of different punch geometries on punch force, the effects of different

punch geometries on cutting surface properties, which is a quality criterion for punching, should also be examined. As a result of the punching process, the different zones of the cutting surface, significantly affect the stretchability of the part. Cutting surface quality is the most important factor affecting the formation of corner cracks. Therefore, the relationship between punch geometry and cutting surface should be determined and the differences in punch forces caused by different geometries should be examined.

For this study, dual-phase steel grade DP800 steel, which is a most widely used AHSS type, were used. Punch with 5 different tip geometries were used for the experimental studies. The cutting surfaces formed as a result of the experiments to be made at constant clearance and cutting speeds have been examined with the help of an optical and stereo microscope. In addition, the punching process will be examined numerically with the finite element method by DEFORM-3D and SIMUFACT-2D programs, and the effects of stress distributions caused by different tip geometries on the cutting surface will be examined. The damage model will be defined for the material and damage constant will be determined. Thus, damage predictability will be provided for the study. Finally, the consistency of the model will be analysed by comparing experimental and numerical studies.

Keywords **:** Dual phase steels, punching, cutting surface quality, mechanical properties. fracture.

Science Code : 91416

ÖZET

Yüksek Lisans Tezi

DP800 OTOMOTİV ÇELİK SACININ FARKLI ZIMBA UÇLARI İLE DELME İŞLEMLERİNİN TEORİK VE DENEYSEL OLARAK İNCELENMESİ

Abdulsalam Abubaker Elamen SAIER

Karabük Üniversitesi
Lisansüstü Eğitim Enstitüsü
Makina Mühendisliği Bölümü
Tez Danışmanı:
Prof. Dr. Bilge DEMİR
Kasım 2020, 66 sayfa

Otomobil hafifliğinin önemi konusunda artan farkındalıkla birlikte, iyi hafiflik, mukavemet ve biçimlendirilebilirlik özelliklerine sahip AHSS çeliklerinin (Geliştirilmiş Yüksek Mukavemetli Çelik) üretimde kullanımı da artmıştır. AHSS çeliklerinin mukavemetinin artması aynı zamanda kesme ve delme gibi üretim işlemlerinin uygulanmasını da sınırlamaktadır. Otomobil üretimi sırasında en çok kullanılan üretim yöntemlerinden biri delmedir. Basit bir süreç olmasına rağmen birçok parametreye bağlı olması, optimizasyon çalışmaları nedeniyle kaliteli çıktılar elde etmeyi zorlaştırmaktadır. İyi kalitede delme işlemi, iki parça arasındaki boşluk, delme kuvveti, delme hızı, pot çemberi kuvveti ve delme ucu geometrisi gibi bazı parametrelere bağlıdır. Delme kuvveti, birçok parametreye bağlı olduğu için bu parametrelerden en karmaşık olanıdır. Kesme kuvvetini etkileyen en önemli parametre, delme ucu geometrisidir. Farklı delme geometrilerinin delme kuvveti üzerindeki etkileri konusunda literatürde birçok çalışma bulunmasına rağmen, farklı delme geometrilerinin delme işlemi için bir kalite kriteri olan kesme yüzeyi özellikleri üzerindeki etkileri de incelenmelidir. Delme işleminin bir sonucu olarak, kesme yüzeyinin farklı bölgeleri, parçanın esneme kabiliyetini önemli ölçüde etkilemektedir.

Kesme yüzey kalitesi köşe çatlaklarının oluşumunu etkileyen en önemli faktördür. Bu nedenle, delme geometrisi ile kesme yüzeyi arasındaki ilişki belirlenmeli ve farklı geometrilerin neden olduğu delme kuvvetlerindeki farklılıklar incelenmelidir.

Bu çalışmada en yaygın kullanılan otomotiv olan AHSS sac çeliklerinden olan DP800 çeliği kullanılmıştır. Deneysel çalışmalar için 5 farklı tipte-geometrili zımba kullanılmıştır. Sabit açıklıkta ve kesme hızlarında yapılan deneyler sonucunda oluşan kesme yüzeyleri optik ve stereo mikroskop yardımıyla incelenmiştir. Buna ek olarak, delme işlemi DEFORM-3D ve SIMUFACT-2D programları üzerinden sonlu elemanlar yöntemi ile sayısal olarak incelenmiş ve farklı zımba geometrilerinin neden olduğu gerilme dağılımlarının kesme yüzeyine etkileri incelenmiştir. Malzeme için hasar modeli tanımlanmış ve hasar sabiti belirlenmiştir. Böylece çalışma için hasar öngörülebilirliği sağlanmıştır. Son olarak, deneysel ve sayısal çalışmalar karşılaştırılarak modelin tutarlılığı analiz edilmiştir.

Anahtar Kelimeler: Çift fazlı çelikler, Zımba ile delme, kesme yüzey kalitesi, mekanik özellikler, kırılma modu.

Bilim Kodu **:** 91416

ACKNOWLEDGMENT

In the name of Allah Almighty Praise be to Allah. The work was carried out in the Faculty of Technology at Karabük University, between September 2018 January 2021 under the supervision of Prof. Dr. Bilge DEMİR, whom I would like to sincerely thank for his encouragement, guidance and advice throughout the period of experimental work and for constructive criticism during the preparation of this thesis.

I am also especially grateful to Prof. Dr. Hakan GÜRÜN for conducting some experiments at Gazi University. I would also like to thank my colleagues Khalil Bin Ras Ali and Abdul Karim Al Zahuqi for their advice and support, and likewise, I do not forget my colleague Mustafa GÖKTAŞ and all the staff in the department for their assistance.

I thank my mum, dad, brothers, and family for their patience and commendable support while preparing this thesis I would also like to extend my thanks to all of my friends and colleagues, and I wish you all success.

CONTENTS

Page

Page

LIS OF FIGURES

Page

Page

Page

LIST OF TABLES

Page

Şekil tablosu öğesi bulunamadı.

SYMBOLS AND ABBREVIATIONS INDEX

ABBREVIATIONS

AHSS : Advanced High Strength steels
TWIP : Twinning Induced Plasticity
CP : Complex Phase
DP : Dual Phase
TRIP : Transformation Induced Plasticity
BiW : Body-In-White
HSLA : High Strength Low Alloyed
HSS : High Strength Steel
TRIP : Transformation Induced Plasticity
TWIP : Twinning-Induced Plasticity
CP : Complex Phase
MS : Martensitic Steel
FB : Ferritic Bainitic
HF : Hot Forming
LA : Low Alloy

PART 1

INTRODUCTION

There were great efforts to decrease the mass of vehicles in automotive industry in order to decrease the consumption of fuel. This is achieved by the use of higher strength steel with great frequency on the structural components of vehicles. Higher strength steel helps to make thinner sections in the car elements that result in lower vehicle mass and enhanced the fuel economy [1]. Recently, dual phase steels are widely used with increased frequency due to their ductility and great strength if compared with other types of steels. The desire is always for higher ductility metal or higher strength steel including magnesium and aluminium, dual phase steel provides the advantages that existed in both previous metals with competitive cost.

Beside ductility and strength, manufacturers seek to save cost in the forming operations. This motivated manufacturers and researchers to search into alternatives to conventional drawings and tamping in automotive industry. High strain rate forming operations is considered one of the most important research areas which witness interest by automotive manufacturing companies. One of these approaches is electrohydraulic forming that is considered a category of forming process which has been studied and searched since the sixties of last century [2]. It is targeted recently due to its popularity to increase the sheet materials formability already used. Electrohydraulic forming provides many advantages such as its requiring to fewer equipment to operate, fewer forming stages and increase the formability of materials already used in manufacturing process. Currently, these advantages are desired in automotive researches. In sheet metal punching process of appliance and automotive industries, the work piece blank is generally equipped by mechanical shearing (which is also called blanking) with high production speed. Operations based on piercing appear in punching the metal sheets to produce geometrical characteristics of final products.

Due to the significance of sheared edge quality to the formability of consequential stamping operations or to the final quality of product, huge amount of researches were performed in classical manufacturing area and huge amounts of literature about mechanical shearing are existed. The sheet metal piercing/flanging has been studied and researched by [3]. This reveals the concerns and problems in the area which involved to the mild steel and low alloy high steel strength and other non-ferrous metals. The main method of the researches and studies was experimental reflection and representation of sheared edges.

In general, the sheared edge includes four areas: roll-over area, burnish area (also called shearing area), fractured (or called ruptured) area and burr area. In many cases, the secondary burnish area may occur depending on the properties of material fracture and blank constraining circumstances. This fast development of new forming techniques, concepts of design, new and good materials enjoy by high solidity and formability has been determined mainly in the automotive sector where the added values of sheet metal parts allow high degree of conducted inventions. Demands to enhance the strength to wright rate resulted in the development of many new types of steels with enhanced strength.

Between the invented types of steels, Advanced High Strength steels (AHSS) are considered the most important of those types which used currently in automotive industry [4]. AHSS are categorized in accordance their crystallographic structure to many types of steels including Twinning Induced Plasticity (TWIP), Complex Phase (CP), Dual Phase (DP) and Transformation Induced Plasticity (TRIP), as shown in Figure 1.1. Besides to what we mentioned above, the third generation of AHSS steels are currently in use.

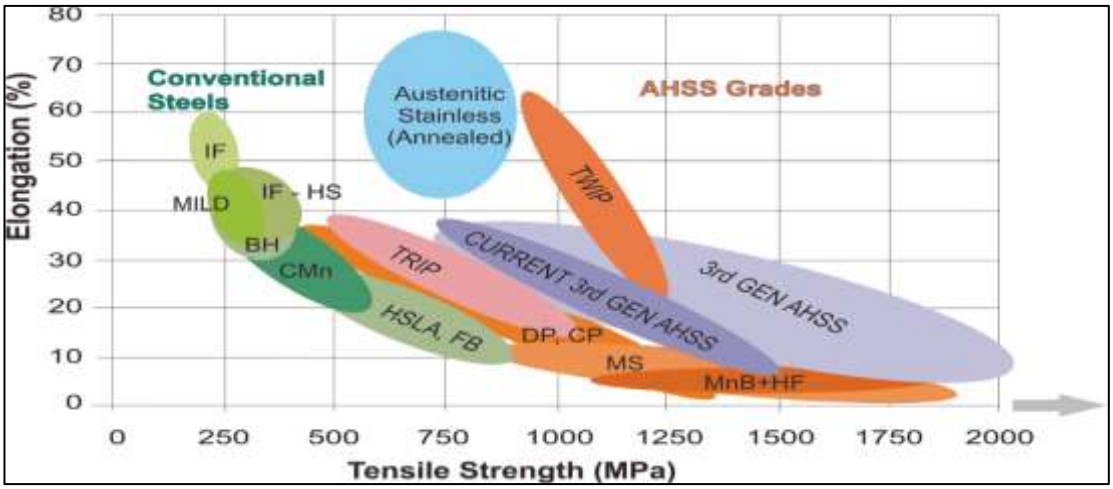

Figure 1.1. Global formability diagram with position of advanced high strength steel [5].

The last few decades witnessed great efforts to develop AHSS and their applications especially in automotive industry [6] and reports on special case studies and researches have been developed by the American Iron and Steel Institute and Auto Steel Partnership [7]. The activities of researches and studies in Europe can be found in a review article [8]. Most of AHSS materials including DP steel enjoy by popular structural features comprising fine-grained martensite particles which are inserted inside a ferrite matrix, produced through special thermo-mechanical processes which result in a good mixture of improved strength and formability with low cost. The family of this materials includes globally unified structure but meticulously highly non-uniform in terms of the presence of DP (or many stages) comprising martensitic particles of a little microns or smaller in their size. In terms of DP steels, by chaining the martensitic volume fraction, many strengths can be gotten in terms of formability better than those existed in traditional high strength steel with similar strength and therefore they entered in many applications. AHSS manufacturing witnesses many challenges and one of these challenges is the difficulty to expect the edge cracking in stamping operations and it is considered to associate with both the structure of materials and mechanically sheared edge properties of the blanks. Therefore, the sheared edges of AHSS must be studied and investigated more and more, characterize and investigate their effect on stamp formability.

The previous studies in this regard consist of AHSS [6] who reported the structural impact on the stretch-flange-formability of three cold-rolled ultrahigh strength steels (with strength at 980 MPa grade) such as one Martensite single-phased steel and two DP steels. The Martensite steel presented the highest hole-expansion rate above the two DP steels. The researchers stated that the gradient of strain in expansion of hole played a significant role. In terms of DP steels, the stretch-flange-formability has been affected by the crack propagation path. A weak formability related with the directing micro-cracking along the interface of stage whereas high formability is related to micro-crack propagation inside ferrite and martensite stage. The most important issue of DP steel in terms of stretch-flange-formability is the difference in solidity [9]. Furthermore, another effected factor is the stage volume fraction. The blanking operation is commonly used to industrialize the sheet metal parts of different materials. Generally, the cut components are subjected to more plastic researches but there are those which directly used in the assembly process of composed products. Many works presented the blanking of components with punch of flat surface have been very well offered as clarified in Figure 1.2 [10].

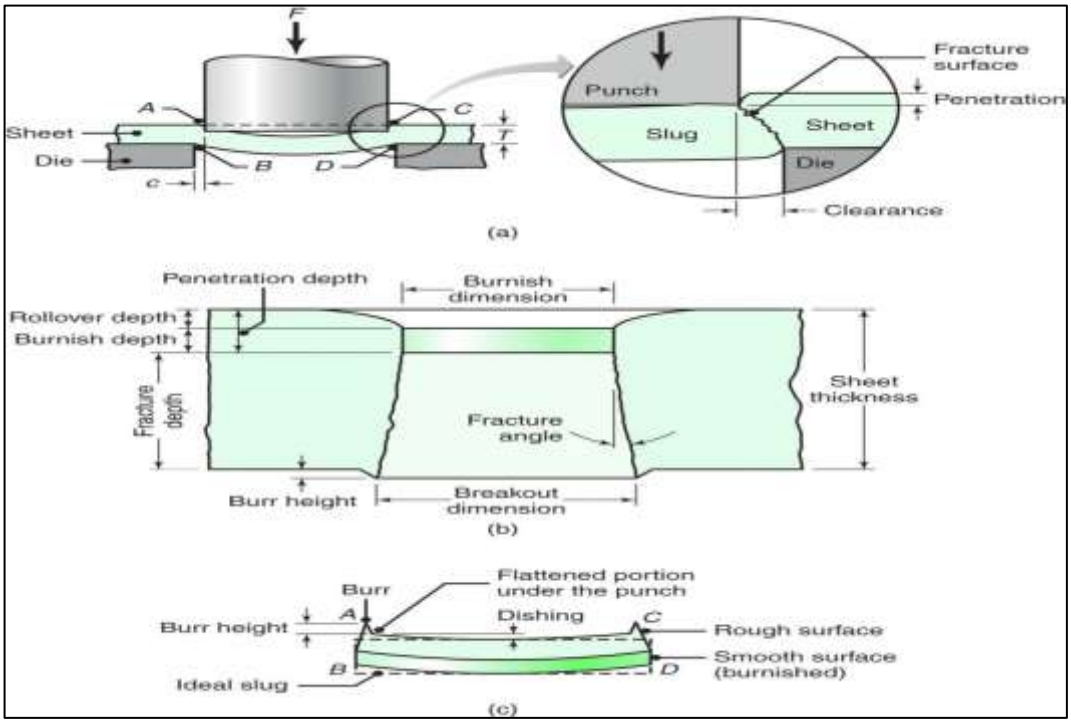

Figure 1.2. (a) Schematic illustration of shearing with a punch and die, indicating some of the process variables. Characteristic features of, (b) a punched hole and (c) the slug [11].

1.1. HISTORY

A consortium of thirty-five sheet steel producers started in 1994, the Ultra-Light Steel, Auto Body (ULSAB)W-1 program to design a lightweight steel auto body structure which may satisfy a extensive range of safety and performance target illustrated in Figure 3.1. In 1998, the Body-in-white (BiW) has been unveiled to validate the program concept design [12] and ULSAB proved to be physically sound, executable lightweight, safe, as well as reasonable. One of the main suppliers to the success of ULSAB was a set of new types of steels and grades which are known as Advanced High-Strength Steels (AHSS) (10). The family of AHSS enjoy by distinctive and unique microstructure using phase transformation and complex deformation processes to fulfil the combination of ductility and strength that never achieved before. The other important feature of these materials is that they use present stamping and assembly fabrication equipment and production approaches [13]. During the following years, AHSS success in automotive industry encouraged steel firms to keep pace their studies and researches on grades and new types of AHSS and then use these steel in different fields of production [14].

DP steel is the pioneer of AHSS that were the first between several candidate alloys systems used in many applications in weight-reduced automotive elements. This is considered a success story in metallurgical. It allows the use of less material to achieve more performance while observing with demanding economic and environmental restrictions. Instead, the huge amounts of literature associate with DP steel demonstrates the immense complexity of structure physics in multi-phase alloys: nearly fifty 50 years after the first studies on ferrite-martensite steels, there are still many open technical questions. Moreover, the last few decades witnessed many development on allowing simulation and experimental techniques expressively enhancing the DP steels understanding [15].

1.2. THE OBJECTIVE OF STUDY

Steel is considered as one of the most significant structural materials and can be developed and used many engineering fields including energy, transportation and

infrastructure. Developments in these fields come by developing AHSS. Strong demands in automotive industry to anti-collision materials fuel effectiveness appears to the scientific and engineering interest of AHSS. DP is one of the oldest identified types of AHSS. However, researches and studies on DP steel have not presented a total understanding to the properties of this material. The complex structure of DP steel increases many scientific questions about this important metal.

This chapter presents the literature on the effect of punches on DP steel and the effect of its unique strength. Like other forms of forming, the application of stamping operations and their modelling by reformulating computer programs with partial elements can offer an outstanding real focus to change and synthesis work and testing work. In written consideration, it can be seen that punching DP steel with special types of punch is not feasible, and the use of imitations will be the first time. To this end, the focus of this research is to hypothetically use testing and limited component strategies to test the punching handles of DP800 steel plates used in the automotive industry. The test complies with EN ISO 14273 measures. The punching process will be conducted with unique staples. The effect of replacing the punching tool on the punching process will be reviewed in this chapter. The experimental and theoretical research on the punching of DP800 steel plates with different punches is reviewed in this chapter. Firstly, it is summarized by showing the features, problems and manufacturing approaches of DP steel. The following sections describe the process of forming metals. Next section presents the results of simulating the FEM process of DP800 steel. Finally, the third part introduces experimental research, stamping in the automotive industry and some mechanical tests on metals that will be used in this research.

PART 2

ADVANCED HIGH STRENGTH STEEL (AHSS)

AHSS are engineering materials which including many characteristic and the most important of them are the combination between excellent energy absorption (crashworthiness), good ductility (formability) and higher strength (performance). Today, the world demand about energy saving, concerns about global warming effect and environmental pollution impacted on the scientific society and associate studies are increasing day by day. The enhancement of strength, materials properties especially metals, capacity, decreasing material cross section, the decrease of part weight and the subsequent decrease in fuel consumption have made possible to decrease greenhouse gas emissions. AHSS is considered the optimal solution for numerous functional requirements of the existing vehicles [16].

During the eighties of the last century, automotive industry faced many obstacles to improve safety, decrease consumption of oil and weight, durability, viability, exhaust gas pollution, fuel efficiency, good formability, environmental policy and quality demands at reasonably low cost [17]. Steel makers agree that AHSS is a new generation of steel which provides very high strength and other useful mechanical properties while stabilizing high capability. AHSS combines between strength and ductility by transformation of phase and solution strengthening and achieve a strength-to-weight ratio at light applications in the automotive industry [16,17]. The steel is classified by the use and carbon content. Carbon steels (0 – 0,30 wt% C) are the most important metal for structure safety and integrity as they structure the car body in White (BIW). The properties of plain carbon steels majorly depend on their content of carbon and microstructure. The main useful impact of these alloying components is increasing strength and hardness besides the hardenability of material. Basically, the stiffness is not stimulated [18].

The quality, microstructural homogenous and low content of carbon for plain carbon steel provide great importance and good formability in automotive industry. However, increasing the strength of vehicle in automotive industry is an important task for the performance issues. Strength can be increased by cold working. Although this is limited due to the chemical structure of the steel. Increase the alloying level will increase the cost and effect positively on the formability. High Strength Low Alloyed (HSLA) steel has been developed to improve the hardness and strength of steel and keep good formability simultaneously [19]. Generally, low alloyed steels include manganese and silicon and may present high strength and good formability simultaneously, if they are first hear conserved to create a matrix of ferrite with islands of martensite [20]. AHSS collects between strength and ductility by solution reinforcement and phase transformation and achieve a strength-to-weight ratio of light applications in the automotive industry.

2.1. CLASSIFICATION OF ADVANCED HIGH STRENGH STEEL (AHSS)

AHSS access into much higher tensile strength if compared with the traditional High Strength Steel (HSS). Strength-ductility relationship is one of the most significant and valued properties of HSS. AHSS includes many types that can be classified according to the mechanical properties of the material and processing. Currently, the most used types of these materials are Transformation Induced Plasticity (TRIP), High strength low alloy (HSLA), martensite (MART) twinning-induced plasticity (TWIP), complex phase (CP), dual-phase (DP), martensitic steel (MS) and Ferritic Bainitic (FB) [21]. Between the properties related to equipped 590R, there are improved formability together with high strength has satisfied wide range of applications in automotive industry. This new types of steel was developed depending on a stable weldable alloy with low carbon levels and alloying components [22]. Bouaziz et al. (2013), keeler et al. (2014) and Kuziak et al. (2008) mentioned that high-definition path and types of AHSSs are families of steels which are stronger and have higher ductility or formability than the traditional HSSs,

There is possibility to differentiate between the AHSS family and the strength levels which can be unevenly defined: product yield strength> 300 MPa and ultimate tensile>

600 MPa. Lower fuel consumption is considered a main element in decreasing the weight of car [24]. Light vehicles have been developed with high quality using high level of steels for example multiphase steels. These consist of perfect selection of DP steels that its structure is consisted mainly of martensite and ferrite to low yield strength applications, high tensile strength, continuous result, and identical elongation need the main materials of AHSS are DP and TRIP steels. Many other types of AHSS have been developed and all of which have structure including two or different stages one of them adds strength and ductility to the materials whereas the others provide more formability as clarified in Table 2.1.

Table 2.1. Advanced high strength steels [67].

	AHSS	**Microstructure Composition**
DP	Dual Phase steel	ferrite, martensite [LLewellyn & Hudd 2000]
TRIP	Transformation Induced Plasticity steel	ferrite, bainite, retained austenite [LLewellyn & Hudd 2000]
CP	Complex Phase steel	martensite, pearlite, retained austenite [IISI, 2006]
FB	Ferritic Bainitic steel	ferrite, bainite [IISI, 2006]
MS	Martensitic Steel	martensite, bainite, ferrite [IISI, 2006]
Q&P	Quenching & Partitioning steel	martensite, ferrite, retained austenite. [Wang & Weijun, 2011

Since TWIP and HF steels sometimes showed improved strength and formability, they are grouped under the heading AHSS [24]. However, they do nor consist a composite structural composition that sets HSLA steels apart from AHSS steels. Furthermore, while the chemical structure of TWIP steels consist of high content of manganese (17 - 24 %), they are not classified as carbon-steels. The microstructure is not the only characteristic which through AHSS can be categorized but they categorized based on the application. In addition, they can be classified based on the mechanical properties,

material thickness and the chemical composition. In Europe, the main feature of AHSS is known as the Euro norm.

2.2. DUAL PHASE STEELS (DP)

This type of steel refers to the group of high strength steels which is categorized into two phases normally a ferrite matrix and a dispersed second phase of martensite, reserved austenite and/or bainite. DP steels have been developed during the seventies of the last century. The motivation behind the development of this type of steels is the need to a new high strength steel without decreasing the formability or increase the cost. Particularly, automotive industry needed grades of steel with high tensile elongation in order to confirm formability [25], high tensile strength to generate exhaustion and crash resistance, low content of alloy to confirm weldability without effecting cost of production. After many years of use, the demand on DP steel is continuous with increase [26]. These types of steels combine between good formability and high strength and therefore decrease the vehicle weights and other products provide economic and environmental benefits. DP steels present higher properties if compared with HSLA. As a result, to the combination between high deformation toughening, good formability, low cost and high strength as shown in Figure 2.1.

Figure 2.1. Example of DP steels as safety details in car bodies.

The most popular method to produce DP steel is by cold rolling of Low Alloy (LA) steels followed by intercritical annealing in a constant annealing line, here denoted to as CAL. The intercritical term denotes to the two-phase field of austenite/ferrite in the

Fe-C scheme. The austenite stage will be transformed into martensite when quenching, delivered the appropriate solidity of the steel and efficient cooling ratio. This will be resulted in a soft continuous phase of ferrite1 with imbedded hard particles of martensite [26]. Figure 2.2 shows the microstructure of DP steels.

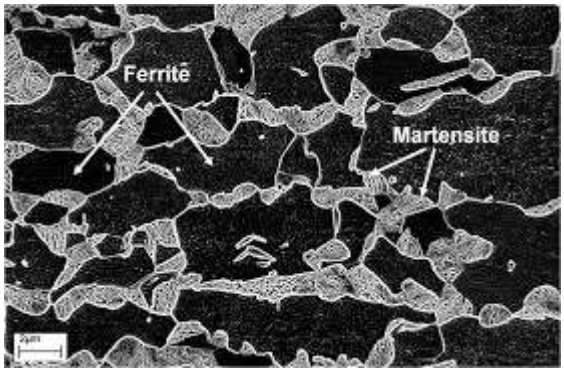

Figure 2.2. Picture of the microstructure of DP800 steel. Using the in-lens detector the hard martensite phase appears as white areas and the soft ferrite phase is dark.

2.2.1. Classification of DP Steels

DP steels include many types including DP 1000, DP 800 and so on according to the eventual tensile strength. The tensile strength of DP steels is over 800 MPa for DP 800 and 1000 MPa for DP 1000 which is greater than the conventional high strength steels that range between 400 - 440 MPa. Nevertheless, they are considered an optimal selection in automotive industry with same production strength [27,28]. So, it can use more than DP sheets which decrease the weight of car without losing their strength. As well as they characterize by higher or similar energy accident absorption. Manufacturers agree that, designing high-level steel-based parts of AHSS provides the chance to decrease the cost of production and vehicle decoration. Presently, DP and TRIP steels are well created as AHSS. Generally, they registered decrease of weight for about 30-40% for 1300-1500 MPa steels [29]. Currently, these properties are included in DP 800 steel and preferred. Furthermore, it is important to get the thermal features of vehicles and other products such as formation, welding, etc. The mechanical properties of DP cold-forming steels change rapidly when the temperature is increased which lead to loss the load bearing capacity of DP-shaped cold steels [28].

Thus, design the structure of DP-shaped steel need knowledge to understand to the thermal properties of the mechanical properties with increasing the temperature. Therefore, it is significant to understand well the thermal properties related to yield strength and DP 800 elastic module with high temperatures. An experimental study has been conducted to analyse the mechanical characteristics of DP 800. Tensile tests have been performed by means of fixed state test approach for temperatures at the range of 20 ^{o}C. Many types of DP steels are shown in Table 2.2.

Table 2.2. Reviews the product property requirements for many types of DP steels, according to ArcelorMittal standard 20×80 mm ISO tensile specimens (thickness: less than 3mm) [30].

Steed grade	Yield Strength (YS) [MPa]	Ultimate Strength (UTS) [MPa]	Total Elongation [%]	Direction
DP450	280-340	450-530	%27	Transversal
DP500	300-380	500-600	% 25	Longitudinal
DP600	330-410	600-700	% 21	Longitudinal
DP780 Y450	450-550	780-900	% 15	Longitudinal
PD780 Y500	500-600	780-900	% 13	Longitudinal
DP800	494-530	800-830	15.4	Longitudinal
DP980 Y700	700-850	980-1100	% 8	Longitudinal

2.2.2. Microstructure of DP Steel

The traditional structure of DP steels includes of the polygonal soft ferrite matrix and that of a 10–40% of the hard martensite island. The strength and ductility of the steel are shown in Figure 2.1. This type of structure helps to achieve the highest tensile strength extending between 500–1200 MPa.

When the volume fraction of the martensite exceeds the 20%, of DP steels that frequently denoted as; the partial martensitic. In order to achieve the personalized requirement, the ferrite-bainite-martensite have been established to modify the mechanical properties. It is detected that bainite instead of martensite improve the formability to little decrease to the development and strength [31].

Martensite fraction effect, spread, size of zone, effect of the ferrite fraction, size of grain of the mechanical behaviour of DP steels have been widely researched and studied [32]. Figure 2.3 gives a clear example on microstructure of DP steels. The soft ferrite phase is shown in white microstructure and hard martensite phase is shown as the dark region.

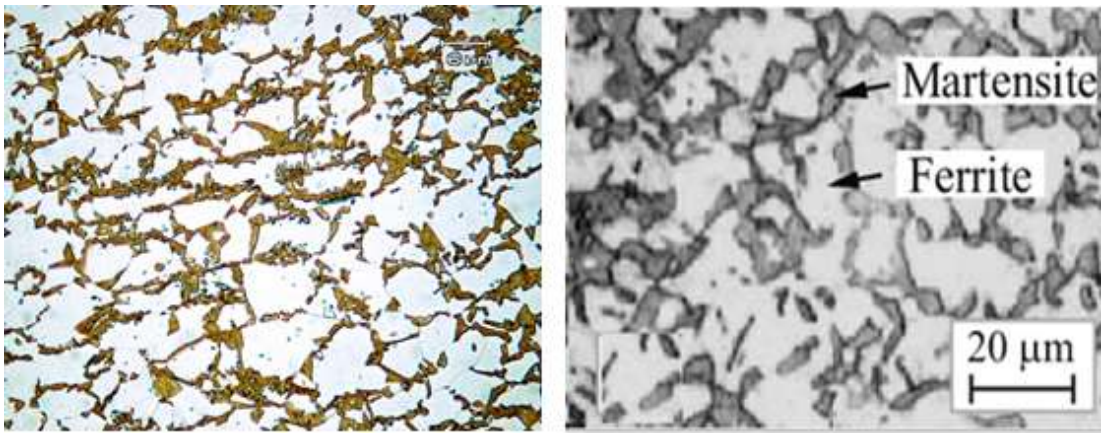

Figure 2.3.The microstructure of DP steel.

Precisely, DP steels started in low or medium carbon steel and it is decreased from the temperature beyond the A1 temperature but under the A3 temperature on a continuous cooling alteration arrangement. Nevertheless, this result is in the structure that includes a soft ferrite matrix which consists islands of martensite as the secondary phase (the tensile strength is increased by martensite increases). Moreover, the comprehensive behaviour of DP steel is controlled by the content of carbon, volume fraction, the grain size and morphology. In order to accomplish these microstructures, DP steel normally consist 0.06–0.15 % C thus strengthening the martensite and the stabilizing austenite phases. The percentage 1.5-3% Mn causes stabilize to the austenite phases and strength in the ferrite. It is supposed that the formation of pearlite or bainite is delayed by the molybdenum and chrome.

The ferrite transformation is promoted by the Si. The reason behind the precipitation strengthening and microstructure refinement are the elements of Nb and V. Furthermore, the distribution of martensite effects the mechanical behaviour of DP steels [33,34].

The martensite regions exist as separated areas within the ferrite matrix results in a further enhanced mixture of the strength and that of the ductility than that of the martensite zones which form a chain-like network structure adjacent ferrite [33]. The refinement of ferrite or/and martensite zones simultaneously enhances the strength and ductility.

2.2.3. Mechanical Properties

The automotive industry needs steel grades with high tensile elongation to ensure the high tensile strength and viability to generate fatigue and crash resistance, low alloy material to ensure that formation will not make an impact on production of cost. Martensite amount phase is considered a significant element control the mechanical characteristics of DP steels; for instance, DP steels have number specific properties such as low yield strength (i.e. 0.2 percent offset), typically high uniform and comprehensive elongation, continuous yielding behaviour (no yield point), high work-hardening rate, high tensile strength (up to 1000 MPa) and [36]. The use of DP steels is continuous and still needed for several years in the future. DP steels have succeeded for many reasons such as combination between high strength and good sustainability and thus, they lead to decrease the vehicles weight and other products have numerous and environmental advantages. As clarified earlier in Figure 2.2 that the comparison between DP steels and HSLA presented that DP steels show better characteristics than others.

The economic demand of fuel reduction in automotive industry encouraged manufacturers to search on new materials to be used between other strategies [37]. The new materials have been evaluated for higher strength or light in order to decrease the vehicles weight have been approximated which result in reducing consumption of fuel. Precisely, TRIP steels enjoy by the demanded ability to absorb more energy

through car accidents due to the deferred transformation of reserved austenite to martensite up on deformation. Combination between strength of TRIP steels, ductility and formability compared with conventional steel can be accomplished by the careful design of structure. The fraction volume, chemical constituent, size and shape of the micro-structural elements principally retained austenite were significant in the tailoring of the mechanical characteristics of TRIP steels [38]. Due to the microstructure, TRIP steels present higher uniform and total elongation with an equal level of strength as DP and conventional HSLA steel which have been clarified. Current researches and studies focus on microstructure, Nugget formation and mechanical characteristics of the AHSS welded resistance particularly on explanation of a single steel grade reply. Similarly, Tong et al [58] examined the mechanical characteristics of DP-spotted steels and their effect on failure behaviour. Nevertheless, the present studies and researches fail to make an accurate comparison between microstructure of spot occurrences and mechanical properties in various levels of AHSS.

2.2.4. Relationship between Ultimate Tensile Strength and Uniform Elongation of Many Steels

The stress strain curves of DP and TRIP steels show high tensile strength, low yield to tensile strength rate, cumulative elongation, continuous yielding and a high uniform as shown in Figure 2.4 [59]. This behaviour can be recognized through the DP steels by the martensite in the ferrite matrix. The martensite convoys by increasing volume because it is shaped through the transformation from the austenite. The ferrite matrix is deformed due to the locally volume increase that led to mobile movements in the interface of the ferrite/martensite, compliant continuous yielding. The hard martensite increases the eventual tensile strength [60]. In TRIP steels distortion through the tensile load causes the reserved austenite to change to martensite. Furthermore, this transformation consists volume extend that result in a partial increase of the strain toughening element. This leads to delay the emergence of necking, higher uniform and full elongation [61].

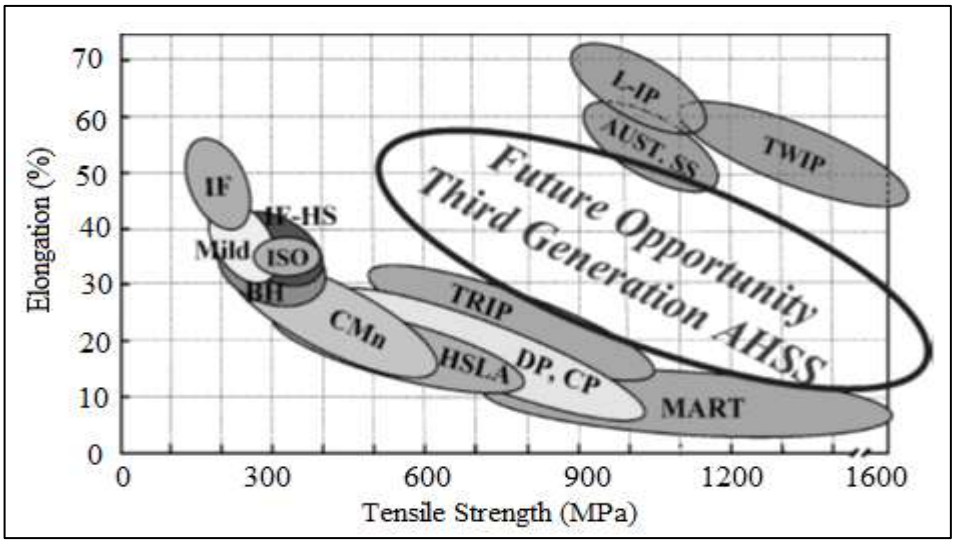

Figure 2.4. Summary of relationship of tensile strength (UTS) and tensile elongation (Uniform) for numerous members of traditional and AHSS [68].

Thus, the excellent mechanical properties in automotive industry include the provision of decreasing the weight of the body, energy efficiency, better passive safety, and good viability. In2007, the regular vehicle had 11.6% of medium-sized and high-trust steel and the entire steel material was 57%. Because of increasing the use of AHSS in different practical applications, the research resulted in enhancing its mechanical performance in fewer amounts. Thus, engineers today face many challenges to select the suitable combination of intensity, ductility, strength, and properties of Fatigue.

2.2.5. Relationship between Yield Strength and Ultimate Tensile Strength for Various Types of Steels (Yield Ratio)

It is important to notice that; the Martensitic MS steels are used in various industries and can be seen in many applications such as of harvesters, ground helmets, cranes, and more. The conventional HSSs including low-level alloy (HSLA) have been existed fro0m more than thirty years and have experience to construct technological base. The users of AHSS asked the quick accumulation of information and distribution because they apply these new types of steels. The strength of total yield and elongation axes present an important challenge. As shown in Figure 2.4, that the steels with high

strength reduced elongation ratio. At present time, researchers and manufactures try to find methods to keep the percentage of total elongation with high strength steels.

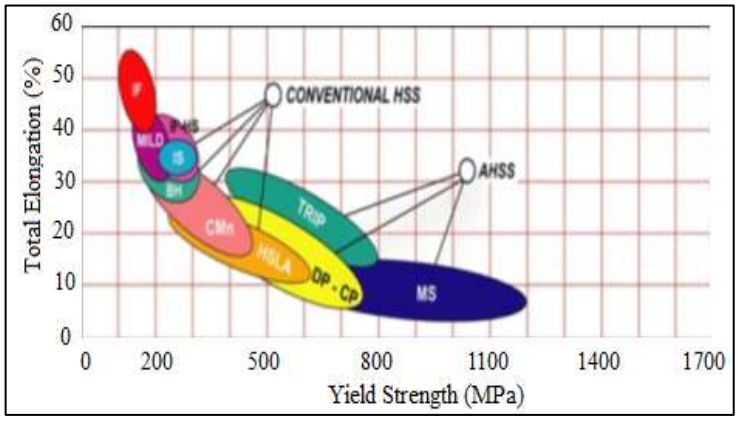

Figure 2.5. Relationship between yield strength and total elongation for many types of steels [19, 38].

2.2.6. Processing of Dual Phase Steel (DP)

In recent years, DP steels development were witnessed great interest in automotive industry. Precisely, the DP steel is produced from a low or medium carbon steel (0.05-0.2 wt. %). This is resulted by the production of steel with potential weight reduction using cheap alloying without losing the mechanical properties. Generally, |DP steel is made up of two phases which are ferrite and martensite. Nevertheless, in addition to the martensite, the DP steel microstructure consists small amounts of other phases including pearlite, retained austenite and new ferrite depending on the thermos-mechanical processing and cooling ratio. The DP steels have been generated by some authors by heating the steel up to austenite in the iron-carbon phase diagram, then direct quenching from temperature over Ac1 temperature (i.e. inter-critical temperature). However, below the A3 temperature on a constant cooling transformation diagram and is reserved to full austenitic microstructure as shown in Figure 2.6. Later, the steel will be cooled to the ferrite + austenite area and stay at that temperature degree and thus, the ferrite can be nucleated at the austenite boundaries. After nucleation, the ferrite produces to the austenite grains. Therefore, the microstructure will be decorated by the ferrite and martensite phases. Also, DP steel has been generated by other researchers based on and derived from the CCT diagram

that covers slow cooling (air) up to the preferred ferrite transformation from austenite and then quenching for converting the continuing austenite to martensite [62,63]. It has been reported about limited works to produce the bainite/ferrite or martensite/ ferrite microstructure of DP steels by first performing laminar cooling then ultra-fast cooling up to coiling temperature and then by coil cooling until the room temperature of hot rolled strip strictly [46].

The DP steel melt is created by oxygen top blowing operation at the converter and it exposes to an alloy treatment in the secondary metallurgy operation [39]. DP steels are produced by many ways and the common way is through the cold rolling of the low alloy steels that is followed by inter-critical annealing in a continuous hardening line. The inter-critical denotes to the two-phase field of austenite/ferrite.in the (Fe-C) diagram. The quenching determines the transformation of austenite phase to martensite and it is provided in appropriate hardenability. The results is the structure of a soft continuous of ferrite and entrenched hard elements of the martensite which has been detected in the study [40]. The martensite will configure lath or plates based on the carbon content in austenite before to satisfying [41].

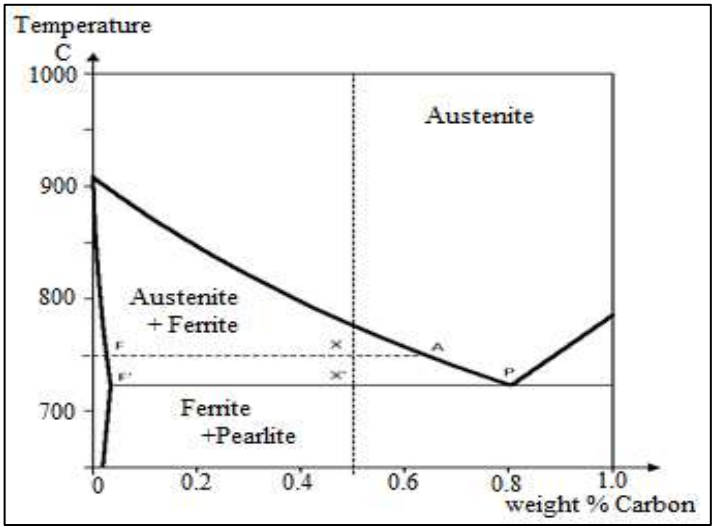

Figure 2.6. Illustration of the lever rule [42].

Many practical applications used the sequential quenching process such as suspension components, bumpers, and wheels. As shown in Figure 2.7 that the intercritical annealing process, is normally used to thin sheets. The primary of the microstructure

of sheet comprises of a ferrite-pearlite mixture that is turned to cold with the preferred thickness. The sheet is heated to the ferrite-austenite area where the suspension of pearlite arises. This process is usually too fast be studied deeply [43]. The dissolution of pearlite with most low carbon steels takes from fifteen seconds to two minutes. Increasing the temperature of intercritical annealing increases the size of austenite decrease the content of carbon for the steel resistance and austenite.

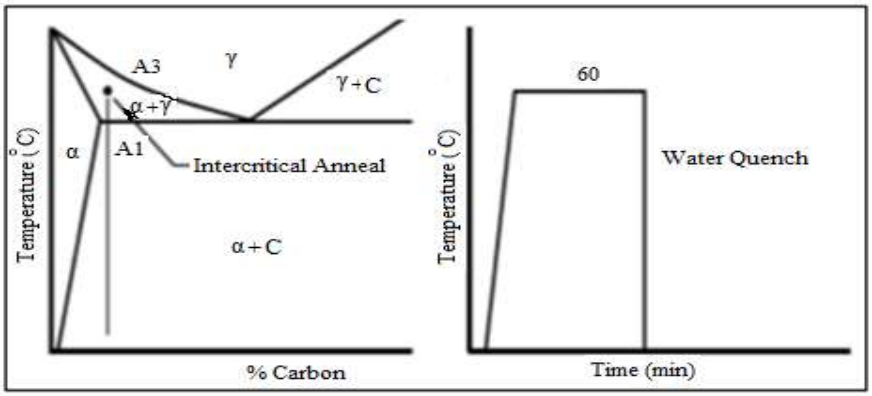

Figure 2.7. Intercritical annealing of DP steel [44].

In general, retained austenite is presented at the edges of martensite islands because austenite reverting to the ferrite by cooling. Ferrite discards the carbon in the austenite because it refrigerates which decrease the martensite finish temperature to be under the room temperature [45]. The comparison of both operations, it can be seen that intercritical annealing operation austenite nucleates and grows at ferrite grain boundaries; in successive quenching, ferrite nucleates and grows at the austenite grain boundaries. The annealing time (holding time) determines the fraction of volume along with the cooling and temperature rate. In the higher annealing temperature, the content of carbon in the austenite will be decreased but the volume fraction of austenite itself will be increased. The intermediate quenching is the third less familiar approach to produce DP steels.

At this operation, the steel must be heated to the austenitic area and held approximately 30 minutes to prove that the microstructure consist of the austenite only. Then, it is quenched to the temperature of the room which forms the total structure of martensitic. The sample must be heated for about 60 minutes in the ferritic/austenitic area to form

ferrite at the particle borders. At the end, it is quenched in order to transform the austenite back to islands of martensite to complete the DP structure [46]. This operation associates DP steel with the content of higher martensite in mineral and mining parts which does not need welding processes.

2.2.7. Dual Phase Steel in Automotive Industry

DP steels is the pioneer of AHSS where the first steels between many candidate alloys systems were to find applications in weight-reduced automobile elements. Instead, this is considered a success story in metallurgical. Lean and simple thermos mechanical treatment allow the use of less materials to achieve better performance and obey to the economic and environmental restrictions. Moreover, the huge literature of DP steels proves the immense difficulty of structures behaviour in multiphase alloys. After fifteen years of the first studies on ferrite-martensitic steels, there are still many open scientific questions which have been answered yet. The good new at this regard is that during the last decades, DP steels witnessed great development that significantly enhanced the concept of DP steels.

Recently, DP steels are commonly used in the automobile manufacturing. Currently, this automation form is increasingly used by the automated people to increase the structural elements of HSLA. The most popular AHSS is the Dual-stage steel (DP) because of many features such as continuous yield and quick working increase, the good viability and ductility with comparatively high strength, non-aging behaviour at ambient temperature and low tensile yield ratio [47][42]. When design with DP steels as with other types of AHSS, the most significant thing that must be taken into consideration is the pressure and increase of baking. DP steels can be developed with a high low tensile yield rate (YTS), allowing a widespread set of applications starting from a crumple area to the structure of body. Occasionally DP steel is chosen to make the body structure and the visible parts including doors, hoods, front and rear railings. also, DP steel is used in more popular applications such as corrugated reinforcements, beams and cross-members, slab, and pillars; cowl inside and out; crush cans; shock towers, fasteners and wheels [48,49]. Figure 2.8. Shows many DP grade applications which are used in automotive industry**.**

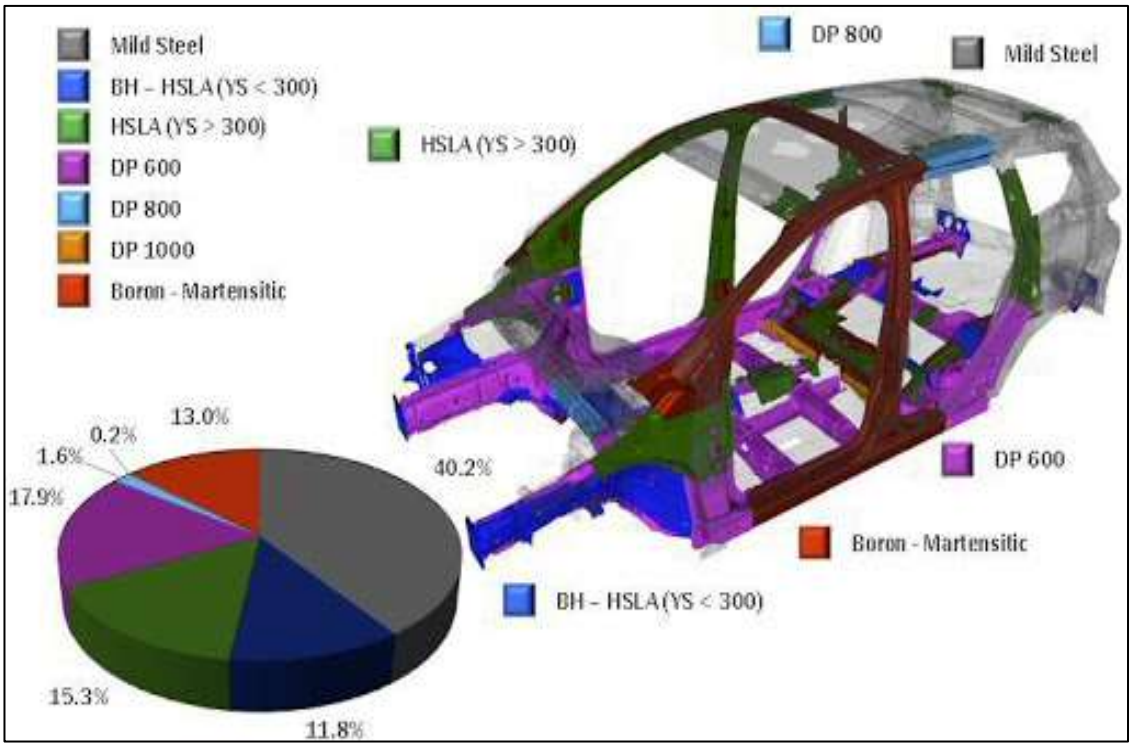

Figure 2.8. Applications of DP steels in automotive industry [49].

PART 3

SHEET METAL FORMING

One of the most significant industrial process is the sheet metal forming. Particularly, this is significant for automobile manufacturing where the sheet metal forming occupies great importance at this position. Automobile manufacturing is the pioneer sector and main driving force in many countries, and it is the main motivation behind the sheet-metal-forming developments.

The competition in car manufacturing is extremely strong leading to larger model variety and shorter model design cycles. The increased competition also leads to a very intense development activity to increase productivity and to reduce costs. Application of light-weight design principles is one of the most important trends to meet the above-mentioned requirements. Obviously, the new design concepts require new materials. The new materials often require new, innovative forming processes and new tooling concepts, as well.

3.1. PUNCHING (PIERCING AND BLANKING)

3.1.1. Sheet Metal Punching Process

In modern industry, the sheet metal punching is considered one of the most popular manufacturing processes. The punching operations may include the occurrence of many failures including tool misalignment, slug jamming, broken tool and tool wear. The previous failures may deteriorate the holes quality or interrupt the monitoring of production line of the punching process is become more and more significant to reveal and correct the failures of punching in time, ensure the product consistence of quality, and protect the tools from destruction. Punching of sheet metal is considered a high transient operation which usually continuous for dozen milliseconds only or even

shorter time. How to efficiently collect experimental data and extract the properties which will illustrate the punching process is significant to the process health monitoring. The force of stamping is considered one of the most significant variables in metal forming or stamping process. Controlling the force of stamping is the efficient and direct approach for control and process monitoring [51].

3.1.2 Punching Operation

The punching is a cutting process through which the material is removed from a piece of sheet metal by applying adequately strong force. The punching operation looks like the blanking except that in punching operation, the removed material is scrap and leaves after the preferred internal properties in the sheet including a slot or hole. The punching is used to create holes and cut outs for many sizes and forms. Punches holes are existed with many simple geometrical shapes (such as rectangle, square, circle, etc.) or combination between each of them. These punches include edges and some of them consist of burrs of not being cut but they are fairly with good quality. Frequently, the secondary finishing are conducted to reach into smoother edges. Each time the punch enters the die, the punching operation removes waste from the metal workpiece. The process leaves hole in the metallic workpiece. The cross-sectional size and shape of the punch regulate the formed hole shape and size in the workpiece [52]. The agglomerates in the holes are dropped into container through a moulding process or recover the agglomerates. When the punch moves upward again as clarified in Figure 3.1, the perforation process is separated into six phases. Please pay attention to the impact of the material when the punch is hit. This effect is more obvious when piercing high-strength materials. The shock wave is high during impact, then begins to flatten, and becomes more controllable as it penetrates. When the punch penetrates the material, the impact load is reduced. The paper may be pulled out. In this case, the peeler releases the paper from the punch of hole. The higher the cutting rate of the paper edge, the better the quality of the edge. When the punch wears out, the frequency of bullets or pull tabs will be higher, and the quality of the holes will be deteriorated [53].

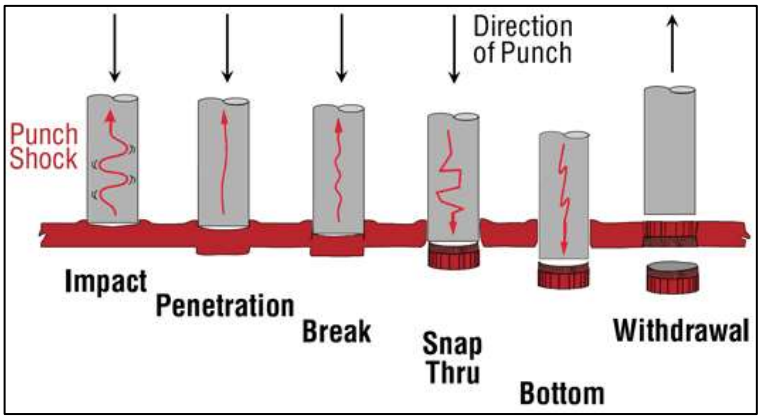

Figure 3.1. During the six-stage progression of hole punching, impact is highest at snap through effect is even greater when penetrate AHSS.

3.1.3. Clearance of Die

The clearance of die is the radial distant between the die and punch as shown in Figure 3.2. As shown in Figure 3.3, the edge is usually characterized by four divisions. If we compare between blanking and punching in mild steel, the selection of die clearance has superior impact of life of tool. Nevertheless, the formation of burr is small and not importantly influenced by changing the die clearance [54]. Increasing the die clearance will increase the fracture area and rollover but less than with mild steel.

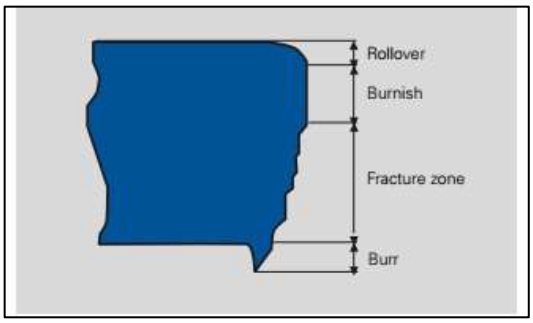

Figure 3.2. Appearance of a cut edge [54].

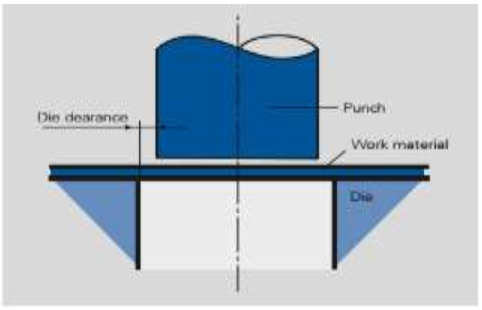

Figure 3.3. Die clearance definition [54].

.

3.1.4. Hydraulic Punch Press

Hydraulic punch presses that power the ram with a hydraulic cylinder instead of the flywheel are either valve and feedback controlled or valve controlled.

Valve controlled machines frequently permit one stroke process permit the ram to stroke up and down when ordered. Controlled feedback systems permit the ram to be correspondingly controlled inside immovable points when ordered. This permits better control over the stroke of the ram and increases punching ratios as the ram no longer has to broad the conventional full stroke up and down but can operate inside very short stroke window.

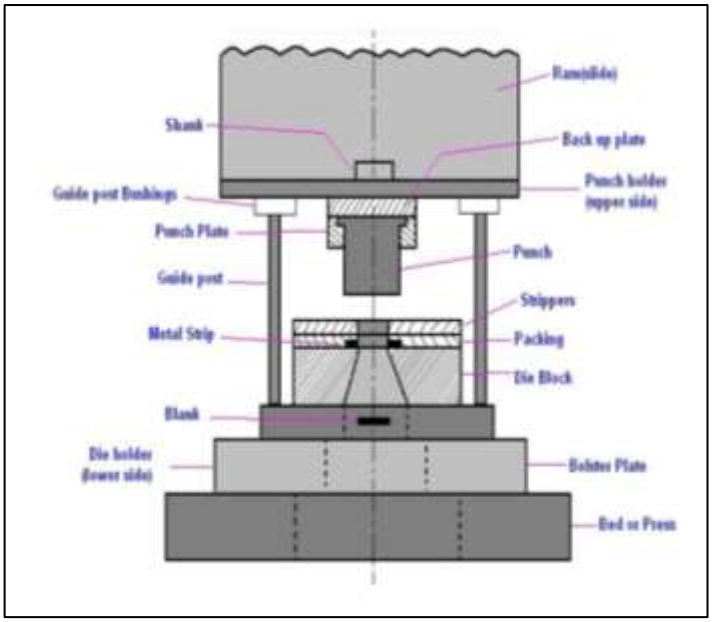

Figure 3.4. Hydraulic punch press.

There are many studies about punching process. A few studies presented below about AHSS and different materials. The one of the most important points in punching/blanking processes are cutting surface properties and punching force. Hence most of studies were made on cutting surface properties and punching force.

Shih et al. [55] In their study they investigated the effects of punches with bevelled geometry on the properties of the cutting surface and hole stretchability of AHSS steels with hole widening tests. As a result of the studies, it has been observed that the cutting force decreases significantly in bevelled punches compared to the flat punch. They also observed that the amount of clearance affects the shear force. As a result of the optimization studies, it has been determined that optimum quality is achieved with 3-degree and 6-degree angle punch, 17% clearance and cutting direction parallel to the rolling direction for AHSS steels.

Myint et al. [56] In their studies, tried to determine a damage constant using different damage models, Cockroft-Latham and Oyane, in order to predict the cutting surface properties in fine blanking process. As a result of FEM studies that was used SPCC material for experimental studies, damage constant C was obtained between 1.39-1.5 for Cockroft-Latham model and 0.9-0.96 for Oyane damage model with different clearance values between 1-25%. It has been observed that increasing the punch corner radius, decreases the amount of shear zone.

Mackensen et al. [57] Used different AHSS steels grade like DP800, TRIP700 and TWIP1000 in their studies, using different parameters to reduce punch forces. In the studies, 5,10 and 15% as clearance, 0 º, 2.5º and 5º degrees as punch angle and 5º, 10º, 15º sheet placement angles were used. As a result, in the experiments conducted with 2.5º and 5º angled punches on different AHSS grades, it was observed that there was a decrease in punch forces around 90%.

Hambli [23], in his study, made a blanking process between 5-20% clearances on 0.6% C metal sheets which has between 1.5 and 3 mm thickness. As a result of his studies, the lowest force was observed at 10% clearance value. In addition, he emphasized that to minimise fracture angle and fracture depth, clearance value should be 5%.

Chiriac et al. [58] in their studies, they punched DP780IBF steel with 6 degree bevelled punch-0 degree flat punch and %15 clearance ,to examine the quality of cutting surface. After punching operation, they made expansion test between %22-27 to investigate cutting surface behaviours. As a result of their study, they observed that different punching parameters can affect the depth and work hardening level. Also, they observed in hole expansion tests that the fracture initiated generally in fracture zone then propagate through burnish (shear) zone to rollover zone.

Behrans et al. [59] in their studies, they investigated the effect of punching speed on punching force. They used AHSS grade DP1000 steel for their studies. After numerical and experimental tests, they reached the conclusion that punching speed does not affect to punching force significantly. They stated the reason of that can be increasing the temperature of cutting locations, correspondingly increase the yield point with the temperature.

Hambli et al. [60] in their studies, they developed a calibration method to obtain reliable ductile damage constant. With this method, the cutting surface properties which has obtained from FEM studies with empirical damage constant, compared with the cutting surface properties obtaining from experimental studies. Damage constant is changed, and FEM analysis is repeated until the consistence is obtained. Consequently, reported that with this method optimum damage constant can be obtained and this method can be used for blanking operations.

PART 4

EXPERIMENTAL STUDY

4.1. GENERAL VIEW

Many manufacturing methods are used to produce DP steel parts, which are commonly used in automobile industry. One of the known methods among these methods is punching. Punching is a very difficult manufacturing method to understand due to complexities in the punching process such as excessive local deformations, high strains and formed temperature. DP steels, which are commonly used in automobile industry, were used in this thesis study. In the study, DP800 sheet steels were punched at certain parameters with punches with different tip geometry. Force graphs were obtained for each punch during the punching process. Moreover, DP800 material model was created and numerical simulation studies were performed on Simufact and Deform finite element programs under the same boundary conditions. The obtained force values were tried to be compared with each other and with experimental studies. Finally, the performance of the punches was evaluated in line with the data obtained.

4.2. MATERIAL PROPERTIES OF DP800 STEEL

For the studies, the commercial DP800 sheet steel of 500x500x1.5 mm was cut t small pieces in 100x30mm dimensions according to EN ISO 14273 standards. The following stress strain curve was obtained from the tensile test performed at 2mm / min jaw speed to determine the material properties. As can be seen from Figure 5.1 stress-strain plot of DP800 sheet steel, maximum stress value is approximately 900 MPa and tough material. Also observed that it exhibited consistent elongation properties.

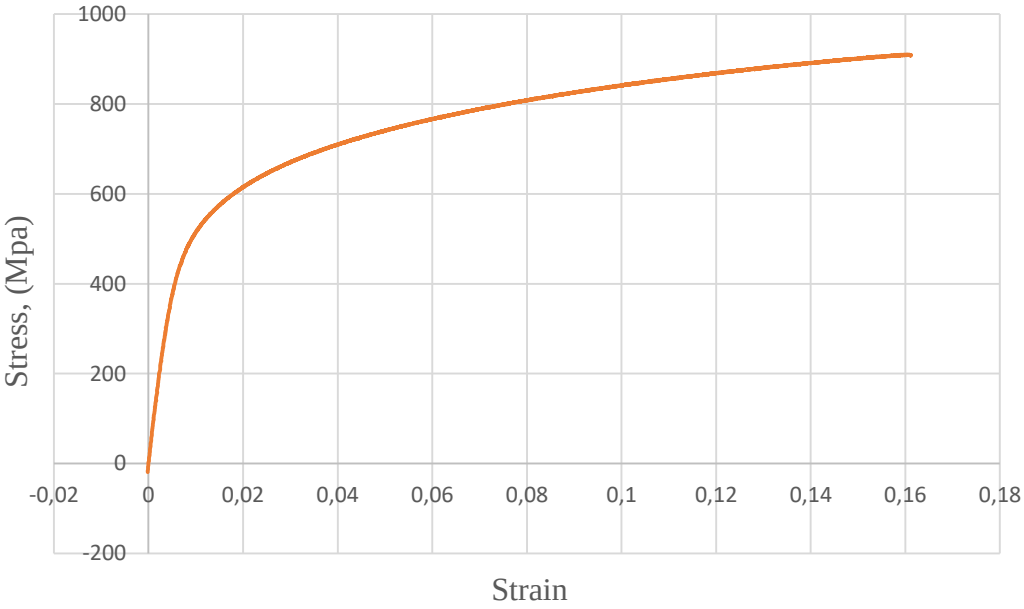

Figure 4.1.True Stress-strain plot of DP800 sheet steel.

4.3. PUNCH GEOMETRIES AND PUNCHING PROCESS

A hydraulic press machine is used for punching operations. The experimental setup integrated into the computer to record force data during the punching process is illustrated in Figure 4.2. As shown in figure 4.2, the force data received through the loadcell with high power capacity were processed through the A / D convertor and recorded via computer software. While 5 different punch types were used for punching operations, the punch speed, and the distance (clearance) between the punch and die were kept constant.

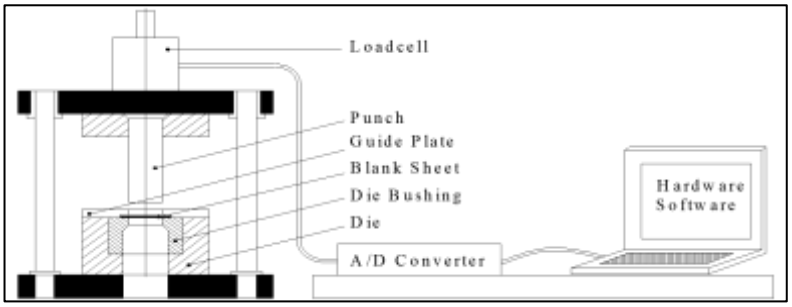

Figure 4.2. Test setup for punching process.

Figure 4.3-4.7 show the technical drawings of punches used in the experiments.

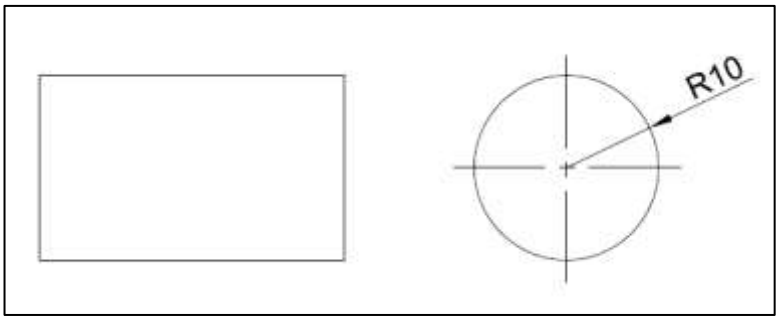

Figure 4.3. Flat type punch.

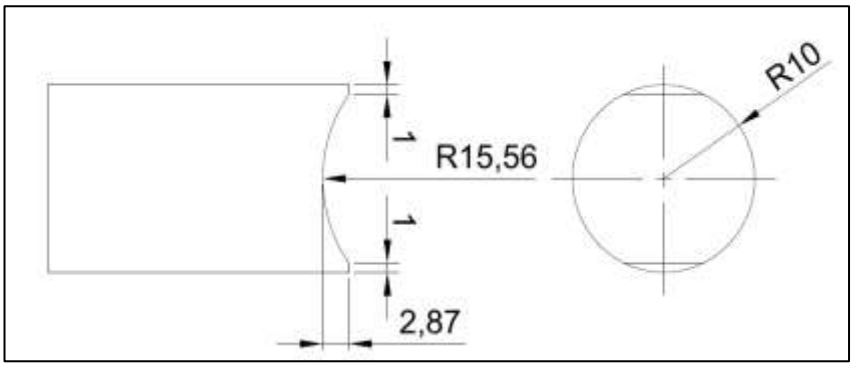

Figure 4.4. Punch with 15.6 mm diameter flute, R1.

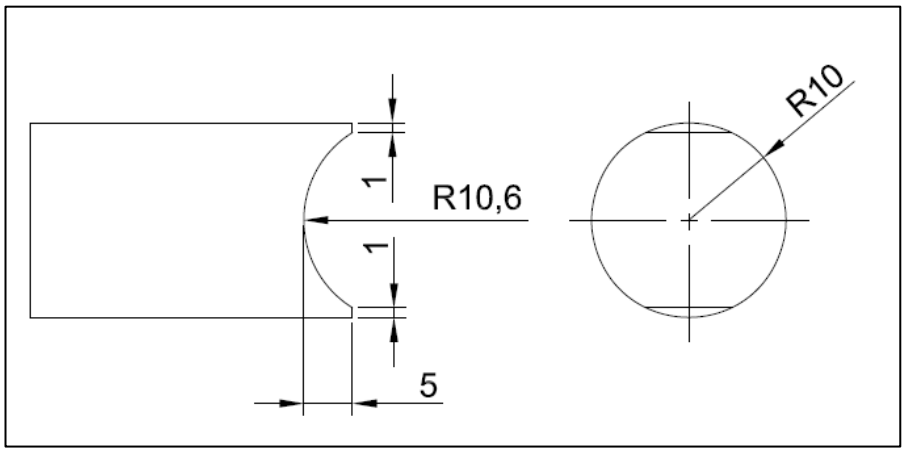

Figure 4.5. Punch with 10.6 mm diameter flute, R2.

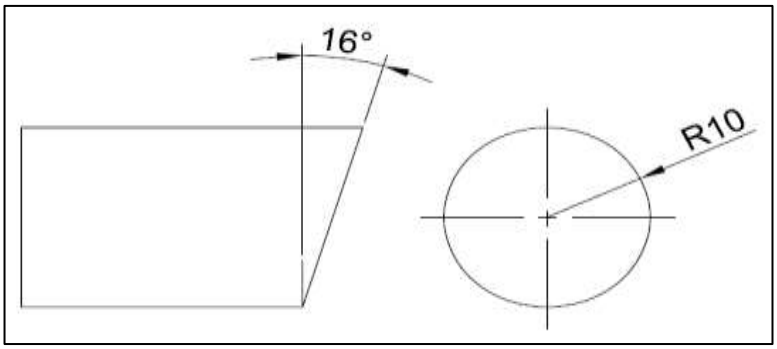

Figure 4.6. Punch with 16 degree beveled tip, P16.

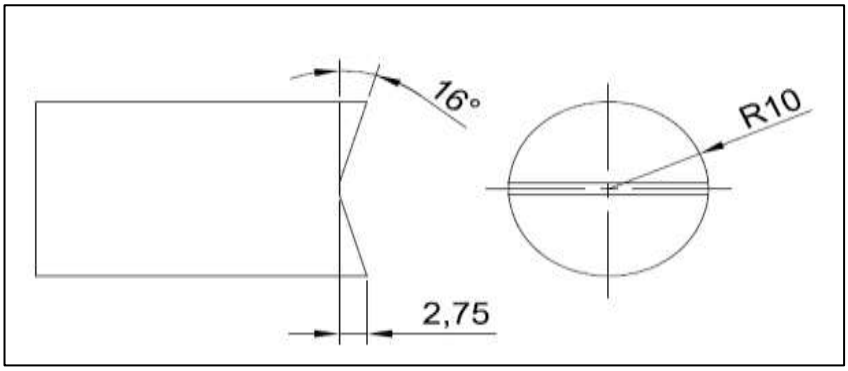

Figure 4.7. Double side 16 degree beveled punch, V16.

Boundary conditions used in experimental and simulation studies are given in Figure 4.8 and Table 4.1.

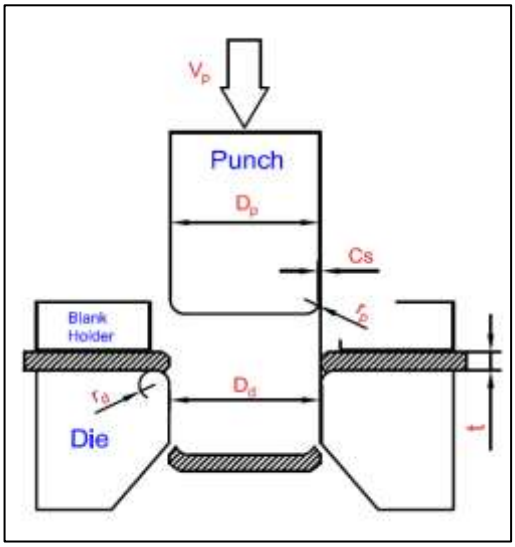

Figure 4.8. Displaying of the parameters that are important for punching process.

Table 4.1. The boundary conditions for punching process.

Sheet metal thickness, t	**1,5 mm**
Clearance between Punch and die, Cs	0,07 mm
Punch diameter, D_p	20 mm
Die corner Radius, r_d	0,01 mm
Punch corner Radius, r_p	0,01 mm
Coefficient of friction	0,1
Press speed, V_p	1,5 m/min

4.4. PERFORMING PUNCHING PROCESSES WITH FINITE ELEMENT METHOD

Punching process is one of the sheet metals cutting processes that are widely used in the mass production industry. Excessive deformation and strain formations make the punching process very complex to understand. Understanding of this complex phenomenon has become quite easy by using the finite element approach. It provides an economical and fast solution to obtain high quality punching processes with finite element analysis. Finite element analysis models with the correct material model are used to obtain extremely realistic data with drilling processes. Most of the studies on this subject have focused on obtaining punch speed, clearance, punch geometry, punch force and hole profiles. In this study, punch geometry and hole profile were analysed by finite element method.

The application and subsequent modelling of punching processes with punching is done by modelling for cost reduction and a comprehensive study as well as experimental work as in other shaping processes. For this reason, the composition of the material used to create the material model, and tensile tests have been conducted with the Simufact program and compared with the experimental tensile test data. Verification of the material model is a very important factor for the precision of the punching process performed by computer. Then, 5 different punching operations were performed in 3-dimensional and 2-dimensional simulation under same boundary conditions and compared with experimental data. Experiments were done by

SIMUFACT and DEFORM finite element analysis programs. Figure 5.10. shows an example model created for the punching process obtained in DEFORM and SIMUFACT environment.

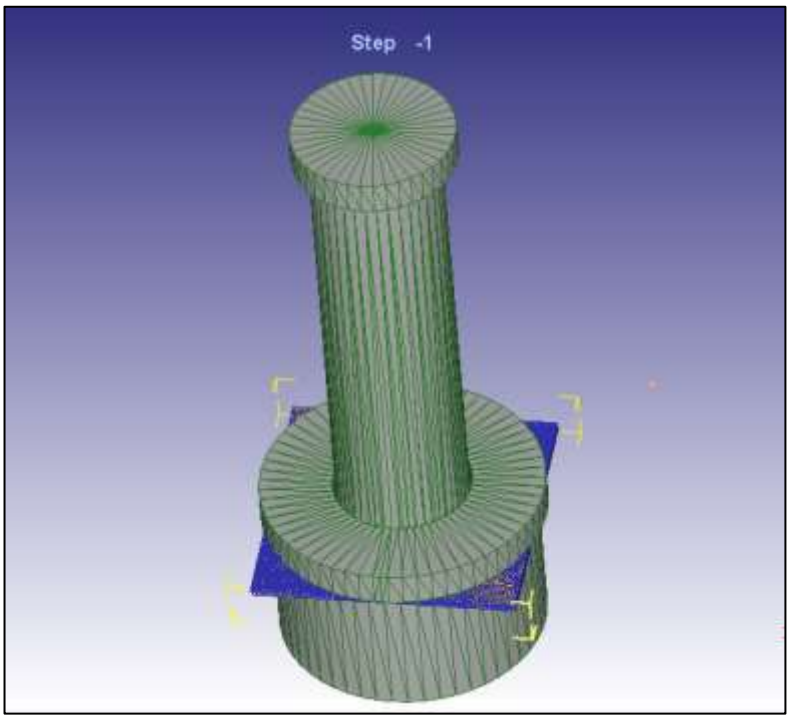

Figure 4.9. The model created in deform for finite element analysis.

PART 5

EXPERIMENTAL RESULTS AND DISCUSSION

5.1. MATERIAL MODEL

Tensile tests were applied to the material model with Simufact finite element software before punching experiments were done. In tensile tests, jaw speed was determined as 2 $mm.min^{-1}$. Stress and strain graph results obtained because of experimental and simulation tests are shown in Figures 5.1 and 5.2. When comparing the graphs, there is a greater amount of strain in the experimental data, while it is thought that the significant difference in the elongation amount of the graph obtained by the finite element approach is because of the meshing process or the inability to model the existing flaws in the material. Besides that, it appears to have similar elongation and bearing load capacity.

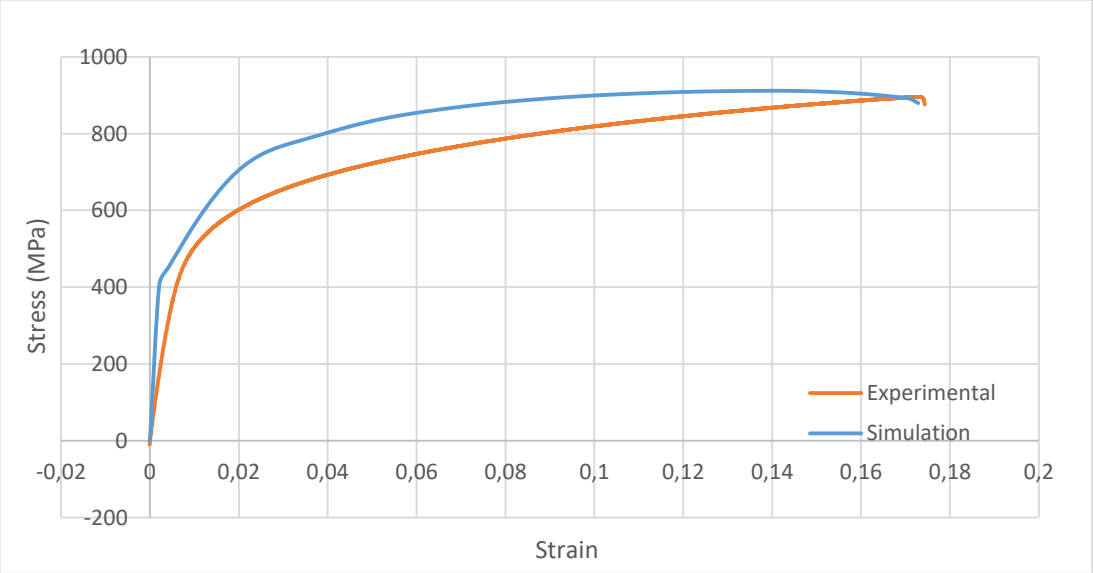

Figure 5.1. Comparison of simulation and experimental data obtained from the tensile test of DP800 material.

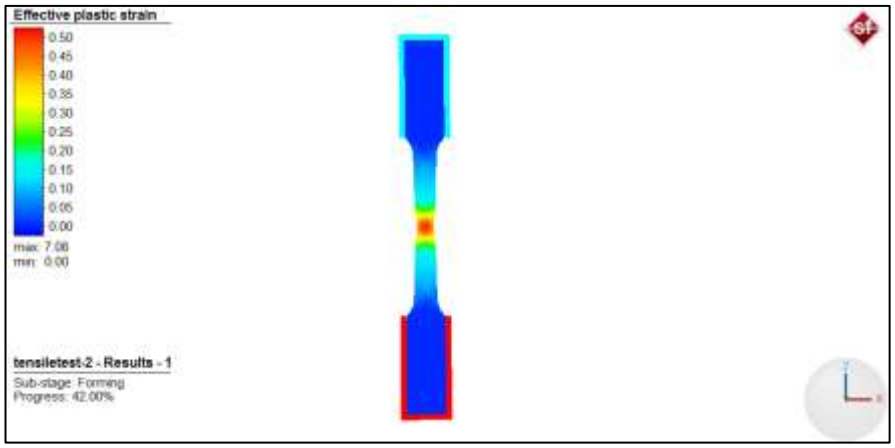

Figure 5.2. Tensile simulation of DP800 sample with Simufact.

5.2. CUTTING SURFACE PROPERTIES

To evaluate the rollover and breaking zones that will occur as a result of the punching process on DP800 steel, 2-D punching processes were performed, and important measurements were made. Although there is a more intense mesh use in 2D finite element analysis, more accurate results can be obtained in less time. It is very important to define the damage model in order to make accurate measurements. Many damage models can be used in finite element analysis. These include many known damage patterns such as Lemaitre, Cockroft-Latham, Oyane, Johnson-Cook, and Gurson. Among these damage model, Cocroft-Latham which is easy to use due to its simplicity and the need for few parameters to use, is one of the most widely used damage models. As can be seen in the formula below, damage occurs when the stress exceeds the determined critical damage constant C. Therefore, with the damage, mesh separation occurs, and the damage can be successfully observed. Myint et al. [15] compared different damage models such as Cockroft-Latham, Oyane and Ayada in their punching studies. They compared the experimental and simulation values to find the critical damage constant and accepted the value showing the same breakage properties as the critical damage constant. Moreover, they found that the critical value of C varies according to the clearance value between the punch and die. Therefore, Cockroft-Latham damage model is used in this study, experimental data and a series of simulation experiment results were compared to obtain the most suitable C constant.

As a result, it has been observed that the critical damage constant C value of 1.5 and around gives similar results to experimental data.

$$\int \frac{\sigma_{max}}{\bar{\sigma}} \dot{\bar{\varepsilon}} dt \geq C \tag{5.1}$$

In the formula σ_{max} denotes maximum principal stress, $\bar{\sigma}$ denotes effective stress and $\dot{\bar{\varepsilon}}$ denote equivalent total strain.

The cutting surface properties obtained after experimental studies with flat punch were examined under optical microscope and measurements of different zones were made. Measurements and surface properties are shown in Figure 5.3.

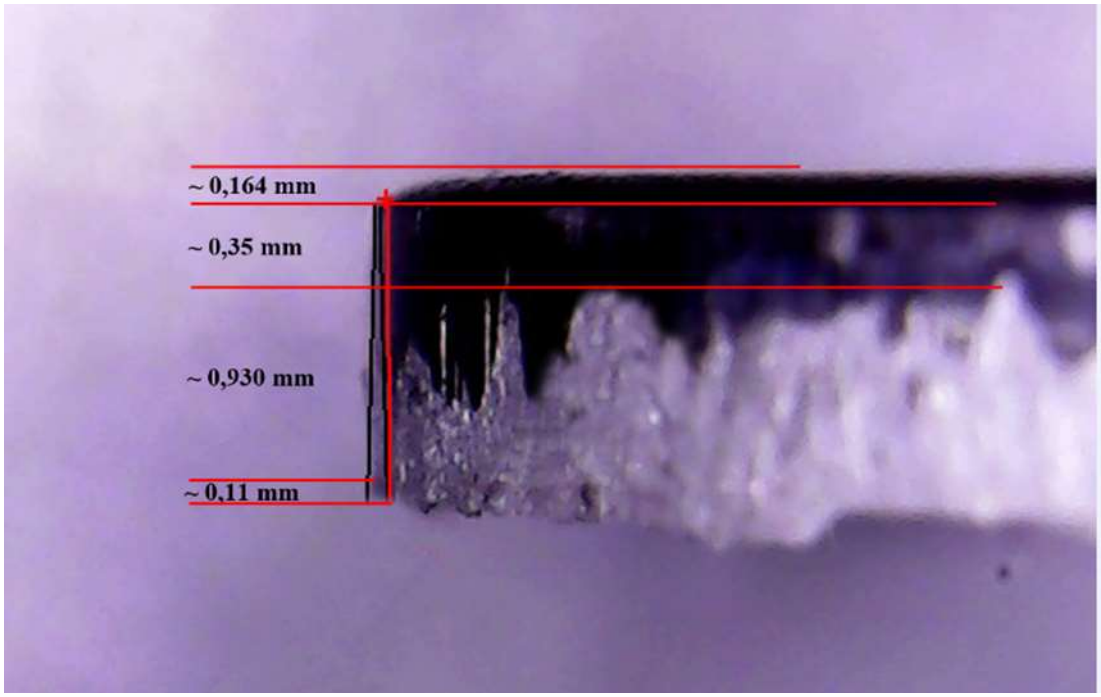

Figure 5.3. Cutting surface image, formed as a result of punching test performed with flat punch.

Cutting surface quality is one of the most important factors that provide flexibility and stretchability during expansion and flanging in the punching process. Therefore, cutting surface quality is very important. According to the surface texture and the cutting surface can be analysis four different region. These areas are burr areas, shear areas, rollover areas and fracture areas. For a good cutting surface, it is desired to

include a large shear area and smaller burr. The ratio of these areas is affected by few elements including material properties, punch corner radius and clearance [61]. Figure 5.3 illustrates the different regions and dimensions of the cutting surface of DP800 steel, due to the 2D finite factor analysis made with the determined critical damage constant values. As can be seen in the Figure 5.4, the shear zone corresponds to 28 % of the thickness.

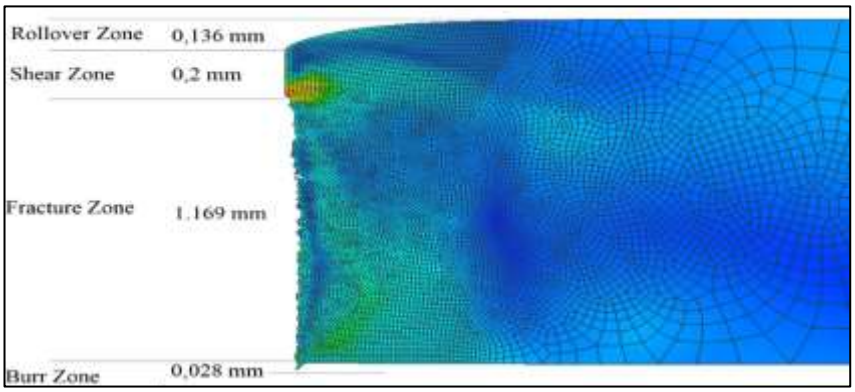

Figure 5.4. The dimensions of the different regions that obtained as a result of 2-D punching simulation by Simufact with damage value of C=1.5.

When Figure 5.3-5.4 are examined, there is a correlation between the cutting surface properties obtained because of experimental and numerical studies. With this study, it was seen that realistic damage occurrences can be predicted in the punching processes of the Cockcroft-Latham damage model. Comparing percentage of cutting surface areas that obtained from two studies are shown in Figure 5.5.

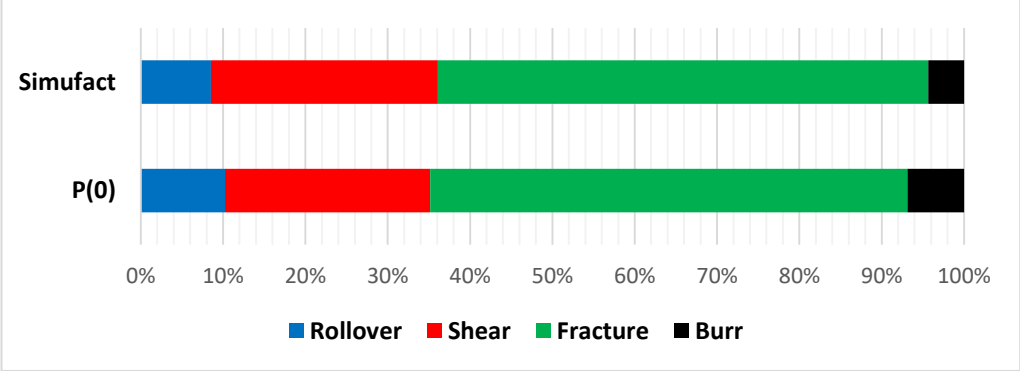

Figure 5.5. Percentage of cutting surface areas observed in experimental and simulation studies.

As can be seen in Figure 5.5, the cutting surface zones measurements are obtained as a result of experimental and finite element studies are compatible with each other. Small differences may be due to the hardening coefficient of the material. This study was able to predict the damage by using the appropriate damage model and finite element analysis under appropriate boundary conditions. However, this study can only be predictive for situations where 2-dimensional flat tip P0 punch is used. 3D analysis is suitable for punches with different geometries that has no symmetry. And more accurate results depend on how dense mesh is used. Increasing the use of mesh can significantly increase the calculation time.

The cutting surface properties obtained result of punching experiments performed not only with flat punch but with different punch types were investigated. When Figure 5.6-5.9 is examined, it is seen that it has relatively different cutting surface properties according to Figure 5.3. Therefore, it can be concluded that different punch geometries affect the cutting surface properties. In addition, clearance also affects the cut surface properties. As the amount of clearance decreases, the cutting zone, rollover zone, fracture angle and burr dimensions increase while the fracture zone decreases. In general, it is desired that the cutting area on the cutting surface be more, and the burr area is as low as possible. This positively affects the stretchability of the hole and the mechanical performance of the perforated part [62]. In some studies, it was mentioned that the cutting surface properties are affected by the clearance and the second burnish area is formed due to the contact of the broken surfaces with each other when the clearance is very low [63,64]. In two dimensional numerical studies, it was observed that broken surfaces touch each other. In punches with inclined geometry, the cutting process is slower on the surface due to the cutting angle, and the crack propagation moves perpendicular to the punch surface according to the inclination angle. In this case, the amount of deformation increases, and the rollover measure becomes greater due to slow shearing [62,65,66]. This situation can be understood from the top view of the rollover regions formed because of punching operations performed with different punches in Figure 5.8. The points where there is an increase in the rollover regions are indicated with a red arrow. In Figure 5.6-5.9, it is seen that the burnish regions of some cutting surfaces formed during punching operations with inclined punch spread throughout the whole wall thickness of the sheet. It has been reported

that this situation may occur due to the shear effect of the inclined punch geometries with the inclination in the progressive strokes and the decrease in the cutting speed [62]. It has been observed that the best uniform cutting surfaces occur in punching processes with P16 punch. Figure 5.6 shows the uniform cutting surface formed during punching with P16 punch.

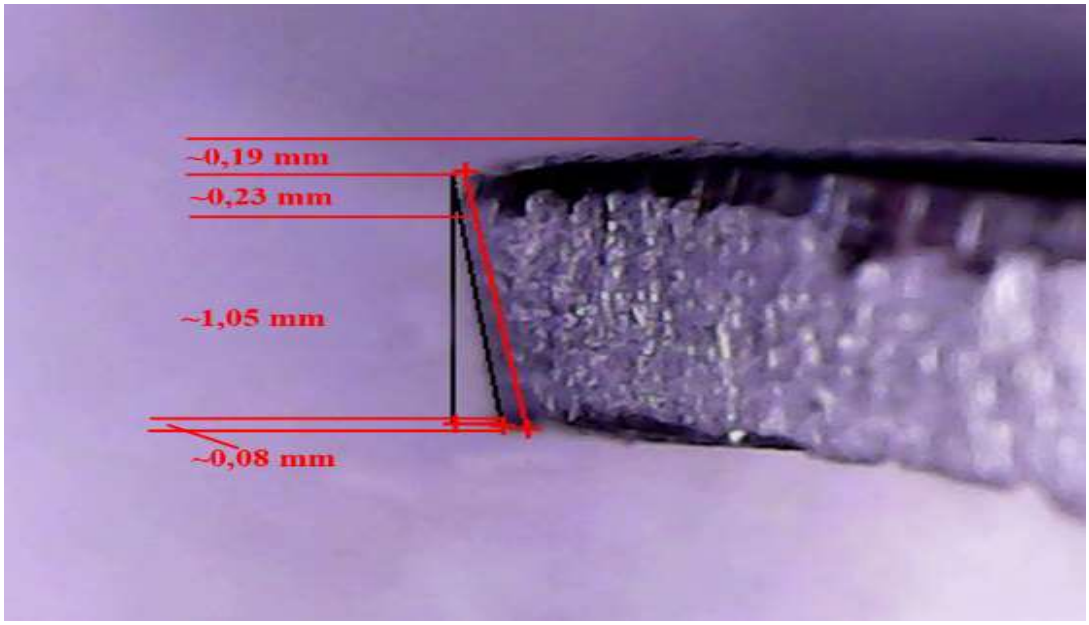

Figure 5.6. Cutting surface image, formed as a result of punching test performed with P16 punch.

As can be seen in Figure 5.8, different punch geometry has significantly changed the cutting surface properties compared to the flat tip punch P0. In this case, as can be seen in the analyzes made with the Simufact program, the tip geometry of the inclined punches may cause different stress distributions due to more stress concentrations. In Figure 5.7, it can be seen that the difference in the upper rollover regions in V16 and P16 punches is sharper than the P0, R1 and R2 punches. It is stated that this situation may be caused by the bending moment caused by tip geometry [63]. In addition to these, when P0 and P16 punches are compared, the reduction in burr sizes can be seen clearly. While the burr size is measured 0.11 mm as a result of punching with a flat tip punch and the burr size measured as a result of punching with a P16 punch is 0.08 mm.

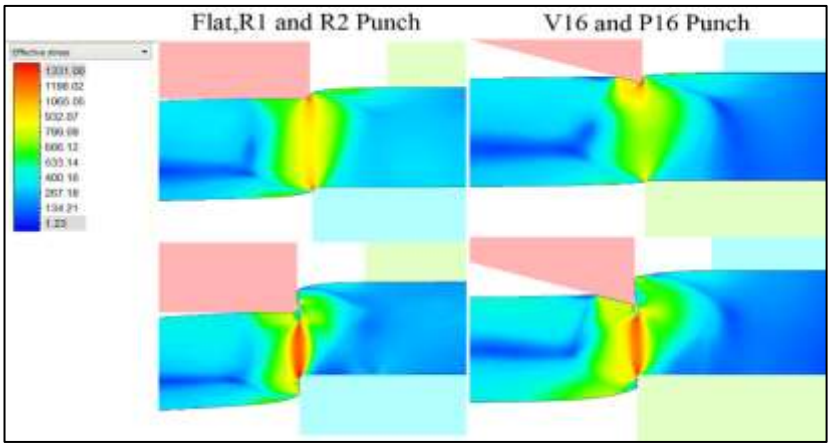

Figure 5.7. Stress distributions of Flat, R1, R2, V16 and P16 punches from Simufact.

The proportional comparison of the cutting surface areas formed as a result of punching processes with P0 and P16 punch is shown in the figure 5.8. As can be seen in the figure, the use of the inclined punch significantly increased the amount of burr, but the fracture zone dimensions increased. As explained above, it is desired that the fracture zone should be less because fracture zone is where the cracks start on the cutting surfaces. In addition, a more uniform cutting surface properties has been obtained in the P16 punch except for the last of P16 punch where the slope is reduced. Hole expanding tests may be the best way to compare these two punches. Because hole expansion tests are one of the most common test methods to determine the quality of the hole created with a punch [67].

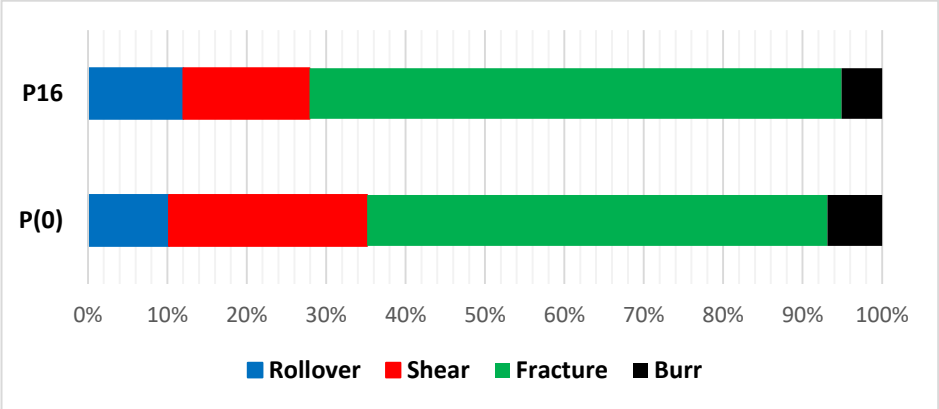

Figure 5.8. The proportional comparison of the cutting surface areas formed as a result of punching processes with P0 and P16 punch.

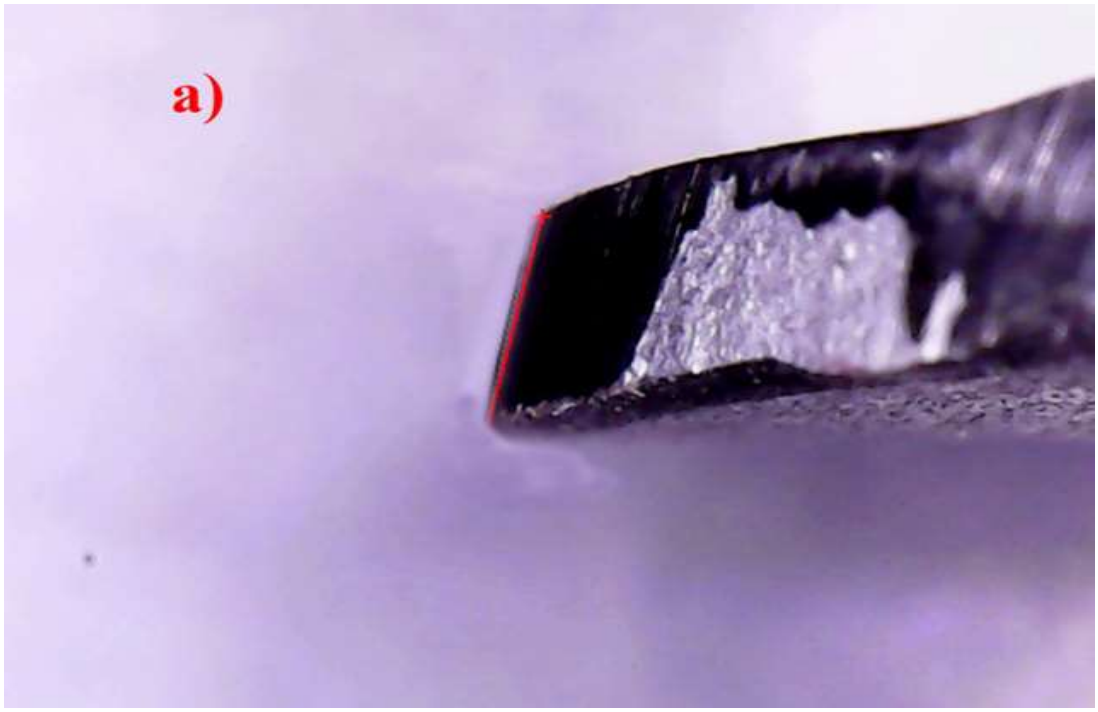

Figure 5.9. Cutting surface image, formed as a result of punching test performed with R1 punch.

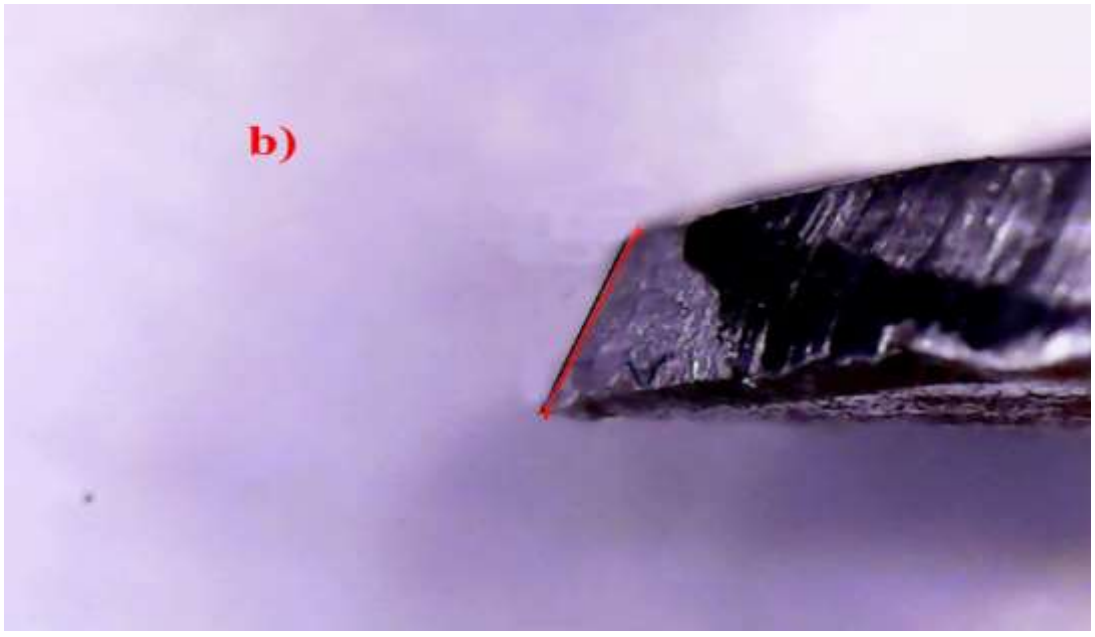

Figure 5.10. Cutting surface image, formed as a result of punching test performed with R2 punch.

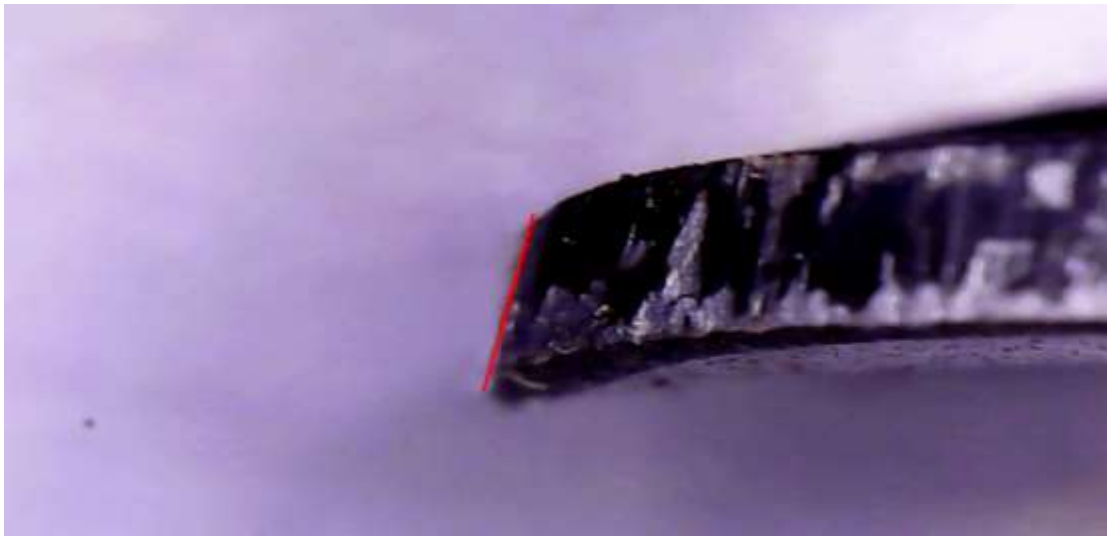

Figure 5.11. Cutting surface image, formed as a result of punching test performed with V16 punch.

Figure 5.12 Show that diameter control has been done in detail by taking measurements parallel to the x and y axes in the hole measurement.

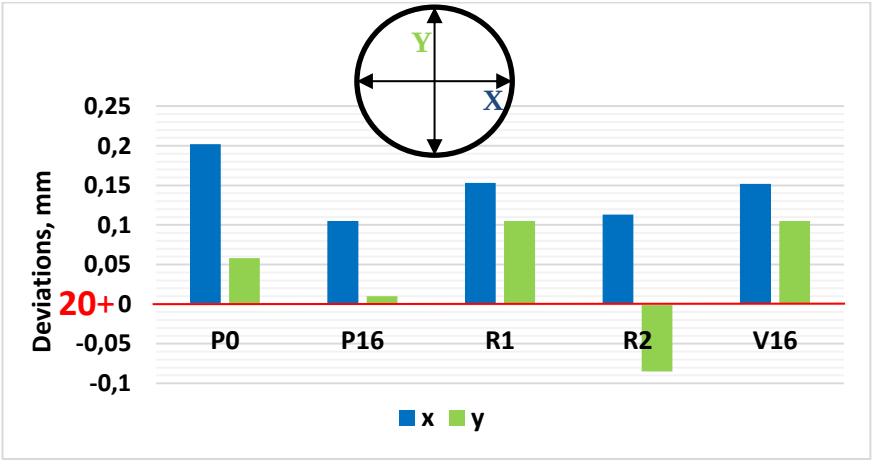

Figure 5.12. The deviations that occur as a result of hole diameter measurements.

When Figure 5.12 is examined, it is seen that the least deviation occurs in the holes formed by the P16 punch. In punching operations with other punches, the highest deviation was observed in the punches Flat, R1, V16 and R2, respectively.

There is significant dimensional difference between holes that punched by different punch that has different tip geometry. So different tip geometry can significantly affect

the dimensional accuracy according to measurements of hole diameters for DP800. Also, [68], in their work, used punches with different angles (3º, 7º and 14º) with AHSS steels. In the studies, deviations were observed in the measurements made with punches with different angles. It has been stated that this is a situation related to spring-back.

Figure 5.13 illustrates the top views of the samples punched with punches with different geometries. Rollover formations and differences caused by punching can be seen the most uniform structure is formed by punching with flat punches and P16 punches. The more severe rollover zone changes can be seen where the first touching point on the part. These points can be seen with red arrow in Figure 5.13 According to diameter measurements, dimensional differences vary between $20^{+0.20}_{-0.08}$ mm for all punches.

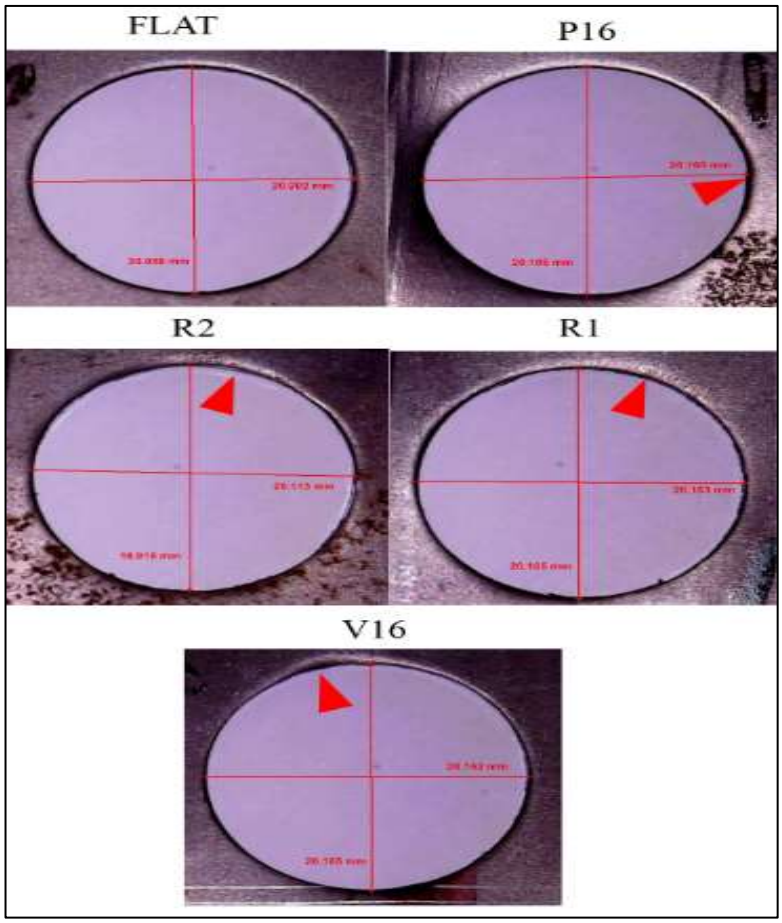

Figure 5.13. The images of different punches of rollover zonal locations.

5.3. PUNCHING (PIERCING) TESTS

The punch geometry significantly affects the stress distributions on the punch process. Therefore, researching punch geometries is a very important issue. In particular, the punch geometry can affect crack initiation and burr zone size. Pu et al. [63] In a comprehensive study on the punching of AHSS steels, they examined punch geometry, clearance, and the effects of the material on punch strength. In the work, they used punches with two different geometries, flat and conical. As a result of their 2D finite element analysis, they saw that different fracture modes were formed. In the process of punching with a conical geometry, it was observed that the combined cutting and bending forces are dominant at the beginning of the crack. It has been observed that better quality cutting corners are obtained in the punching process made with a conical punch.

In this thesis, 5 different punches were used that have different geometry. According to the 3D finite element analysis, the tip part that penetrates the part first in the R1 and R2 punch at the beginning of the punching process shows similar stress distribution with the flat punch. With the increase in penetration, the cutting angle formed according to the size of the flute diameter increases and the cutting angle decreases towards the end of the flute, then the force increases again, thus completing the punching process. In addition, for R1 and R2 punches, there is a significant correlation between increasing cutting angle and punch forces. It can be seen that the punch force reduces when increase the cutting angles.

Contact angles for different punch geometries are shown in Figure 5.14. The red regions show the areas where the punch touches, while the blue regions show the non-contact areas. It is observed that the highest cutting angle during cutting occurs in the R2 and R1 punch.

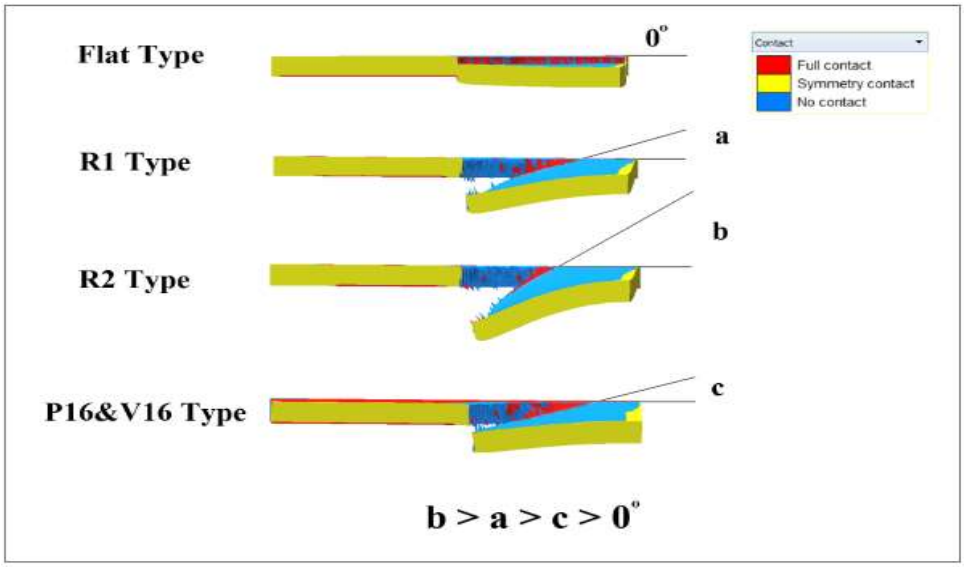

Figure 5.14. Comparison of cutting angles obtained from finite element analyzes with different punch geometries.

The reason for the difference in force arising from V16 and R1 punches is thought to be caused by the fact that the two flat surfaces in the R1 punch geometry significantly affect the punching force. As shown in the results gotten from the 2-dimensional finite element analysis in Figure 5.14., it is seen that the tip geometry importantly influences the stress spreading and crack initiation perpendicular to the part thickness.

As a result of punching experiments, different punching forces were observed with punching geometries. Especially, it has been observed that there is a significant correlation between the contact surface and the punch force according to the finite element analysis and experimental studies. It has been observed that in the punching process with an angle of 16 degrees, the contact point with the punch tip penetration follows the punch circumference by deformation and fracture, so that during the punching process it has less contact surface area, and the cutting angle is high, the minimum punch force is obtained from the punch with 16 degrees incline. It was observed that the highest punch force occurred in the process of punching with a 0-degree flat tip punch, where the highest deformation per stroke occurred. It has been observed that there is an equal amount of deformation around the punch tip during punching. After the R1 punch is observed with the first contact, maximum deformation is observed, as the contact point moves from the flat area to the other inclined areas, it

exhibits a deformation behaviour like the punch with 16 degrees inclination with the effect of the cutting angle, so the punch force decreases, and the punch force increases again at the end of the stroke. Similar deformation properties were observed in the operations performed with the R2 punch, while it was observed that it had a more inclined middle surface due to its smaller diameter and therefore more cutting angle, and therefore it fell to lower forces. On the other hand, in the V16 punch, a deformation similar to that of the punch inclined 16 degrees is observed, and the relatively low inclination that increases the cutting angle, the more contact area and the ending in the centre of the punch, relatively higher punch force has been obtained. The different stress distributions showed in Figures 5.15-5.19. These stress distributions also represent the punch contact. The figures numbered 1, 2 and 3 denote the beginning, middle and ending of the punching processes. As can be seen in inclined punch stress glide around the punch according to the punch geometry. As seen in Figure 5.15, the first contact of the flat tip P0 punch is shown in case 1. As the stroke continues to increase, the part remaining under the punch takes the shape of a concave due to the formation of bending moment and as seen in the 2nd case, the contact becomes concentrated around the punch tip. As the stroke continues to increase, the material rises above the yield point and, as seen in case 3, the stresses concentrate on the part then, separation and rupture occurs.

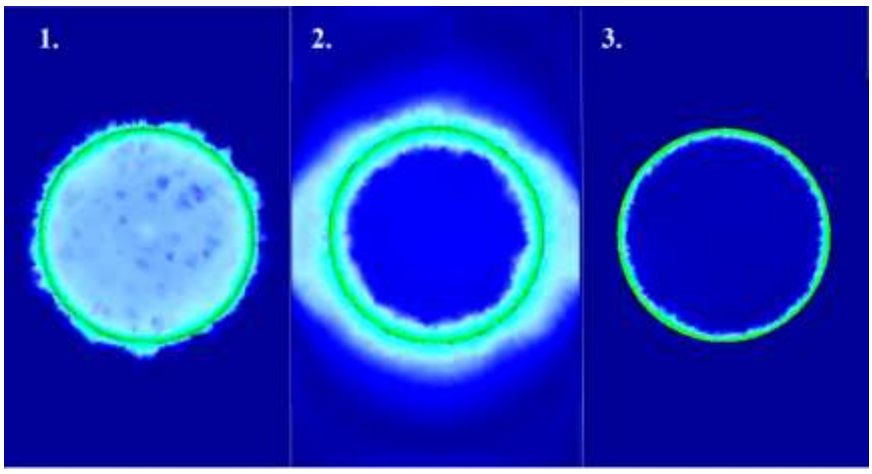

Figure 5.15. The stress distribution during flat punching process.

As it is seen in Figure 5.16, when the tip of the beveled punch touches the part, the stress concentrates and as the stroke continues, starting from the first contact area, the

resulting stress passes over the material yield strength and rupture occurs. With the case 2 and 3, the contact moves around the inclined punch tip with increasing stroke and the tension gradually increases on the material. In case 4, the contact slides towards around the punch tip and finally process is completed with increasing stroke and the stress concentration on the material is concentrated again locally at the rear. Then rupture occurs. The flow direction of the contact is shown by the white arrows. Therefore, with the increase of the contact stroke between the punch and the part, the contact does not occur all over the punch and creates a force-reducing effect. Although the pour point of the material is constant, the force decreases as the contact area decreases

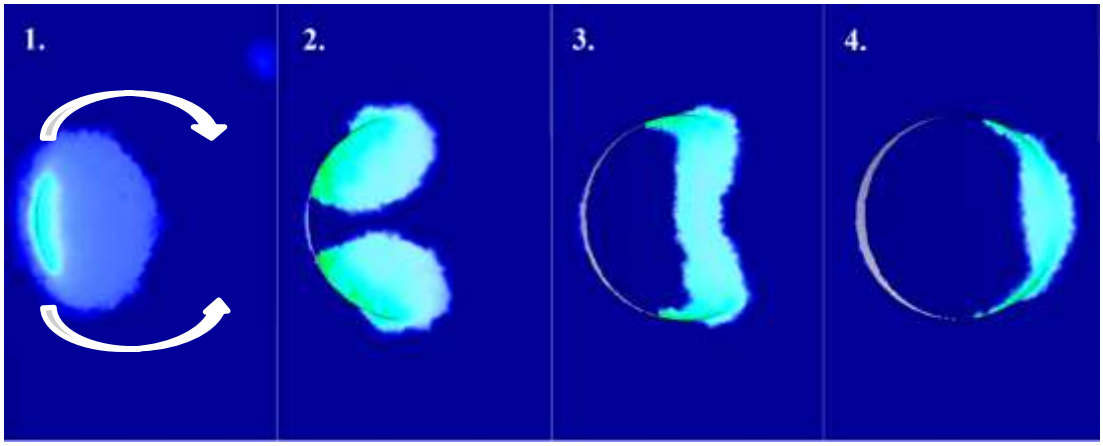

Figure 5.16. The stress distribution during P16 punching process.

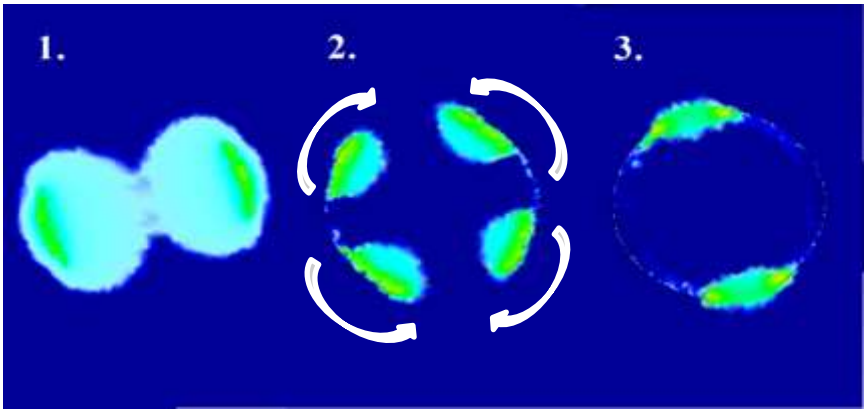

Figure 5.17. The stress distribution on part during R1 punching process.

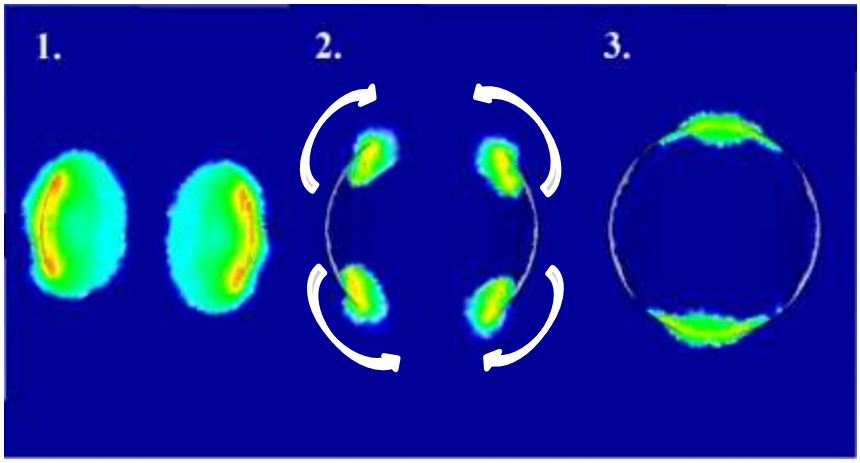

Figure 5.18. The stress distribution during R2 punching process.

As seen in Figures 5.17, 5.19 since there are no transitional surfaces similar to R1 and R2 punches in V16 punch, contact flow travels more uniformly around the punch.

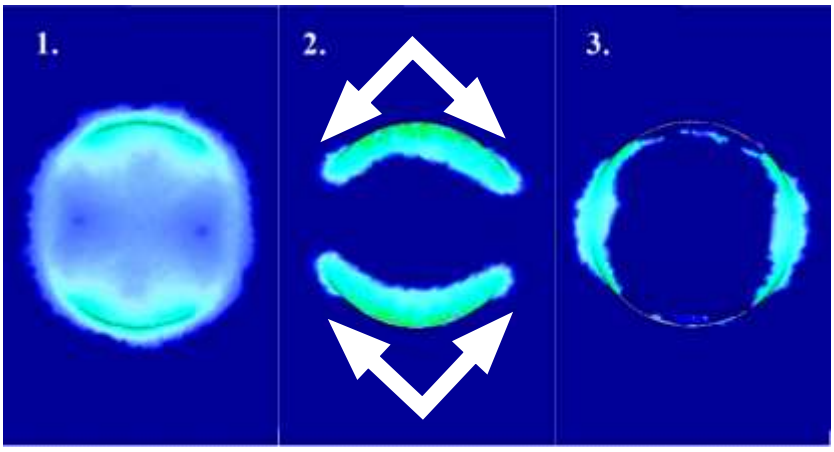

Figure 5.19. The stress distribution during V16 punching process.

As can be understood from the figures, punch tips with different tip geometries cause different stress and strain distributions. Punching forces obtained from different punches are given in Figures 5.20 -5.24. The highest punch force was observed in flat punch, while the lowest force was obtained in P16 punch. As can be explained in previous pages, punch angle is significantly affecting the punch force because of contact area and force relation. Lower forces were seen on the R2 punch due to the difference in angle between the R1 and R2 punches. Although the V16 punch is the double-sided version of the P16 punch, the obvious difference is that the angle in the

middle of the punch is 0, and the contact areas are occurred more than the P16 punch, hence the punch force is higher in the V16 punch.

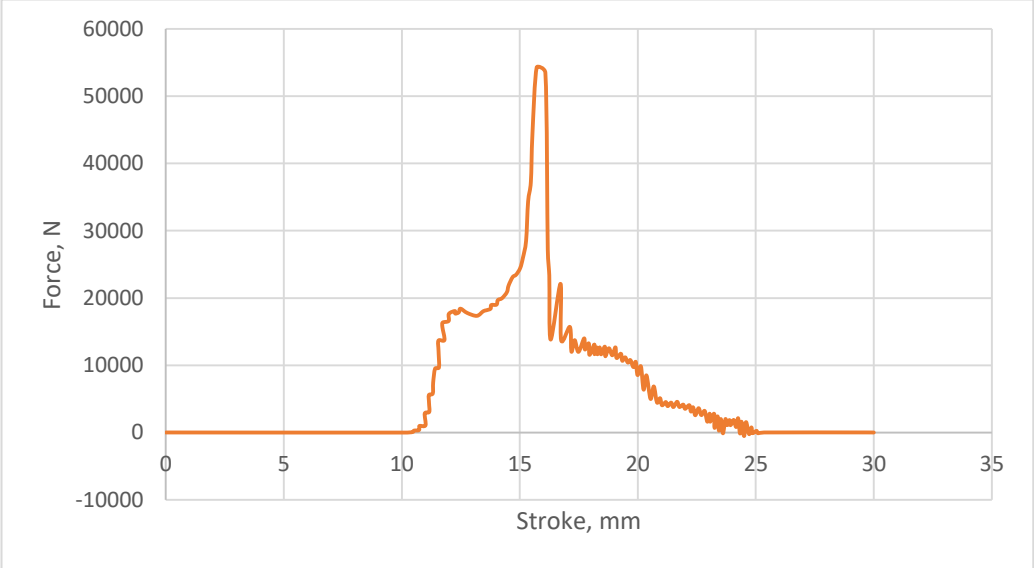

Figure 5.20. The force graph obtained from punching process made by flat punch.

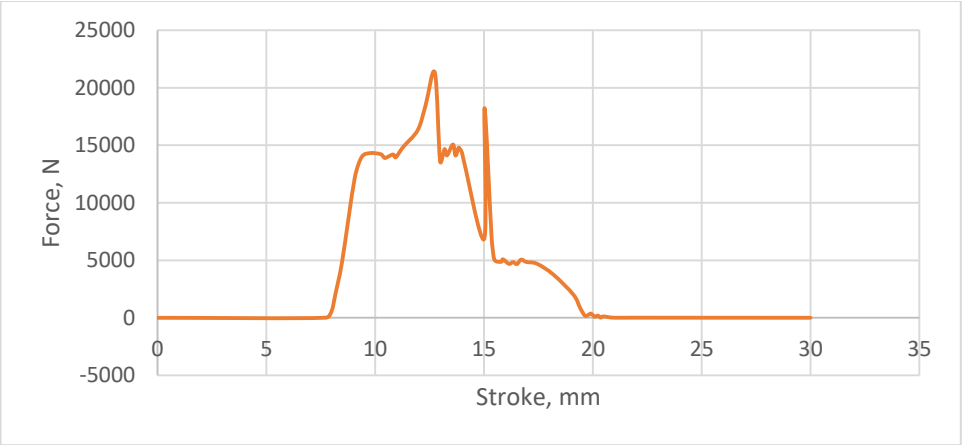

Figure 5.21. The force graph obtained from punching process made by R1 punch.

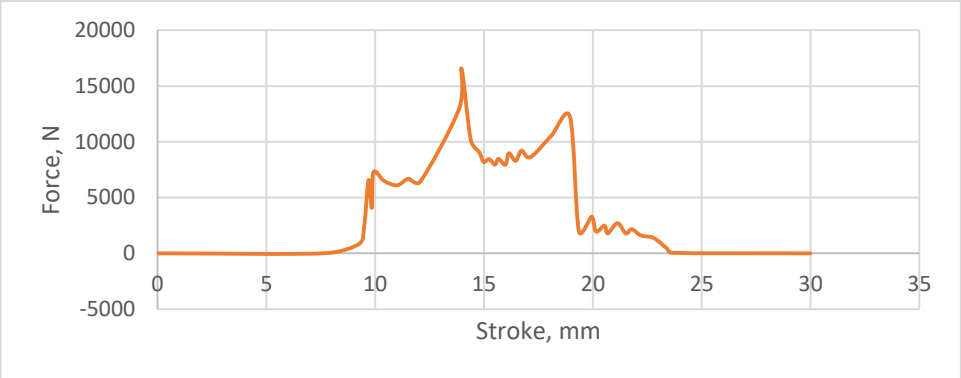

Figure 5.22.The force graph obtained from punching process made by R2 punch.

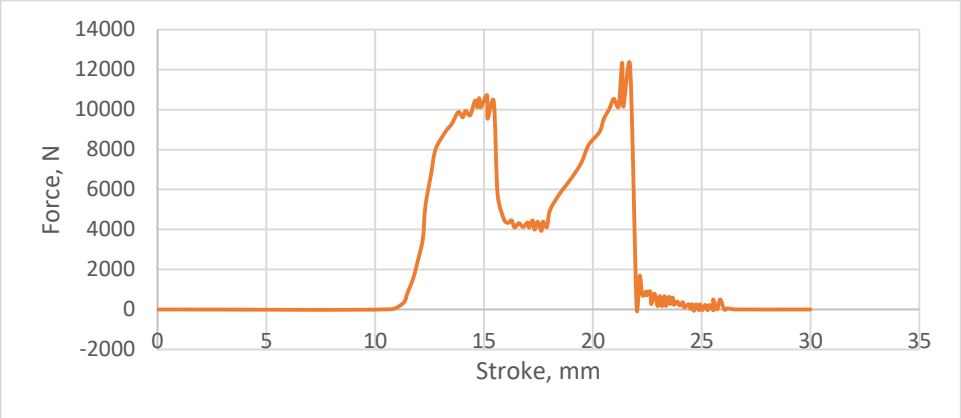

Figure 5.23. The force graph obtained from punching process made by P16 punch.

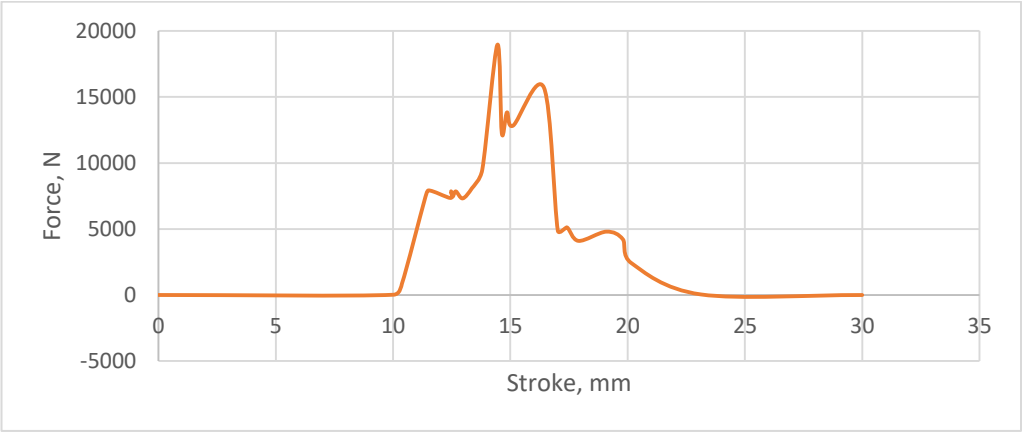

Figure 5.24. The force graph obtained from punching process made by V16 punch.

The experimental results obtained by using five different punch shapes and DP800 sheet material have shown that the cutting force is significantly affected by the punch form, as seen Figuer 5.25. It was found that the maximum cutting force value was

obtained with Flat punch as 54302 N. The other cutting forces were obtained as 12298, 16523, 12171, and 18953N in the use of the punches named R1, R2, V16, and P16, respectively. Consequently, it is very clear that the cutting force is much higher when using Flat punch type and sharply decreases with the use of the other punches.

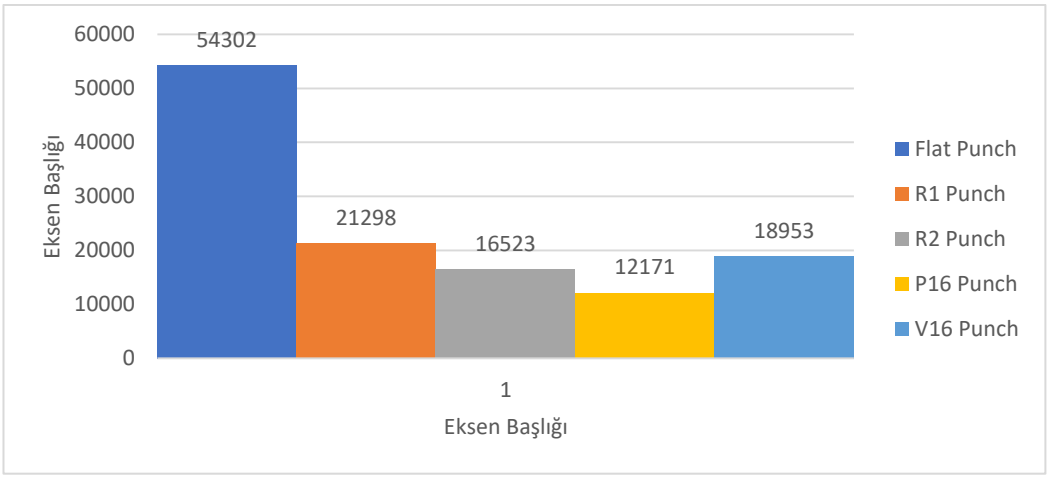

Figure 5.25. The force values obtained from punching process made by different punch.

Analyses/simulations were carried out using Deform software. The 3D models were used in the analyses to ensure the consistency with experimental studies and to see the performance of the software on the simulation of punching operations. The analyses obtained using 3D models for cutting of DP800 sheet material by flat (0), curved (R1), and angled (P16) and Double side degree V16 , which are given in Figures. 5.26-5.30

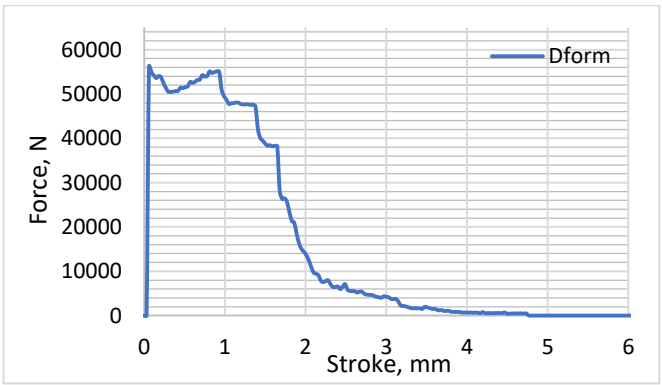

Figure 5.26. The force graph obtained from punching process made by Flat Punch with DEFORM.

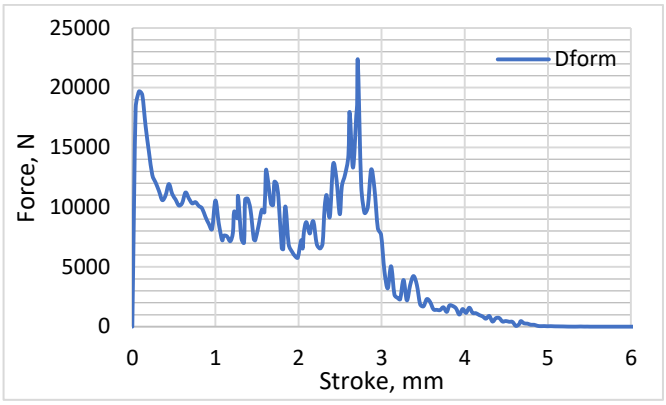

Figure 5.27. The force graph obtained from punching process made by R1 Punch with DEFORM.

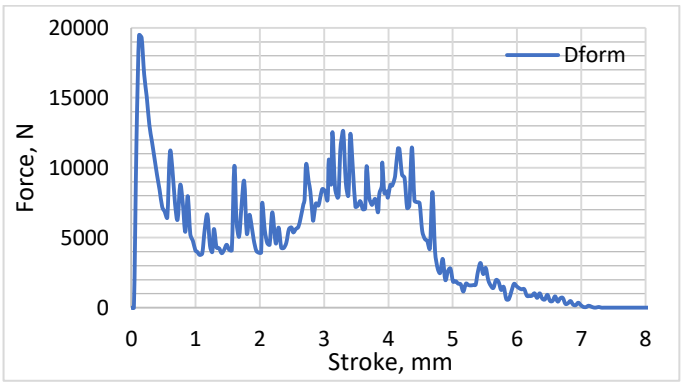

Figure 5.28. The force graph obtained from punching process made by R2 Punch with DEFORM.

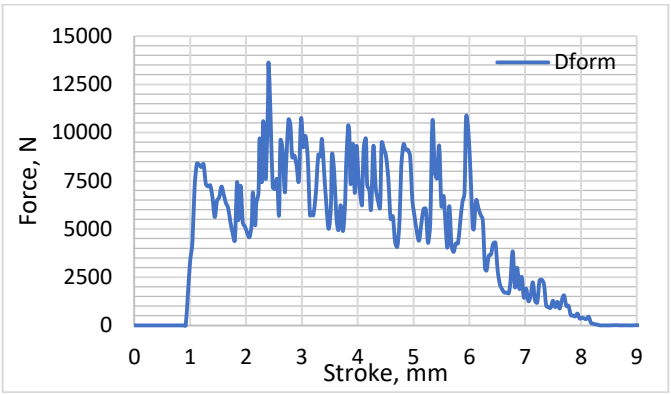

Figure 5.29. The force graph obtained from punching process made by P16 Punch with DEFORM.

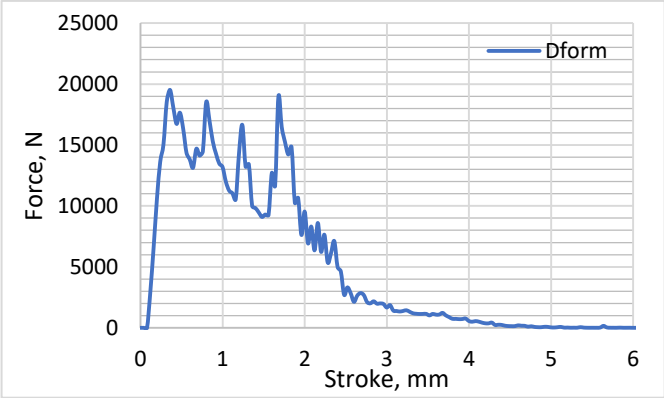

Figure 5.30. The force graph obtained from punching process made by V16 Punch with DEFORM.

As a result of the theoretical studies conducted by using Deform Program, it was seen that the results were very similar to the experimental ones. The maximum cutting force obtained from Deform Program is 54943 N for the Flat punch , and experimental result is 54302 N for the same punch. Similarly, the maximum cutting forces were obtained as 22000 N and 21298 N for the punch R1, 18000 N and 16523 N for the punch R2,13635 N and 12171 N for the punch P16, and 19522 N and 18953 N for the punch V16. The first given values refer to the Deform results, and second values are the experimental results. The results obtained from the deform program and experiments are given in Figuers 5.26-5.30 according to the punches used. A comparison of the cutting forces obtained from Deform program and experiments, in cutting of the DP800 sheet material by all the punches used is given in Figures 5.31-5.35

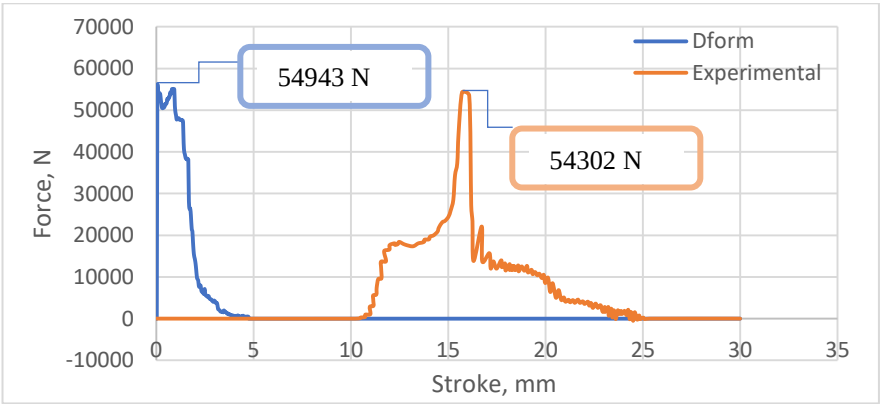

Figure 5.31. Comparison of the graphics obtained from the experimental and simulation punching process made with flat punch.

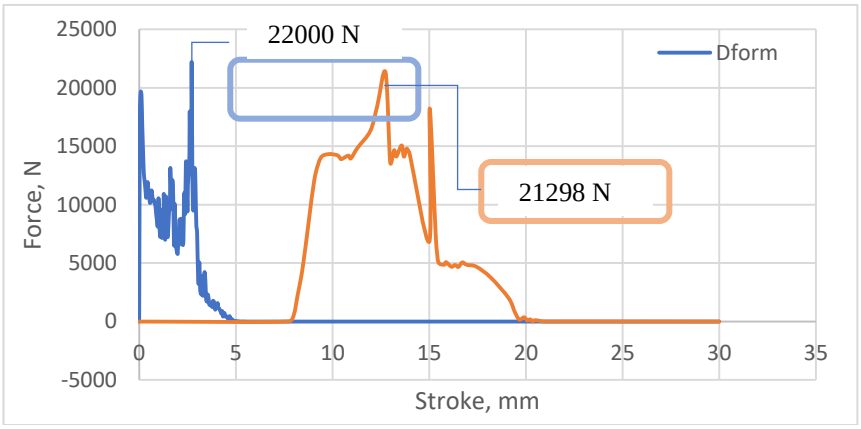

Figure 5.32. Comparison of the graphics obtained from the experimental and simulation punching process made with R1 punch.

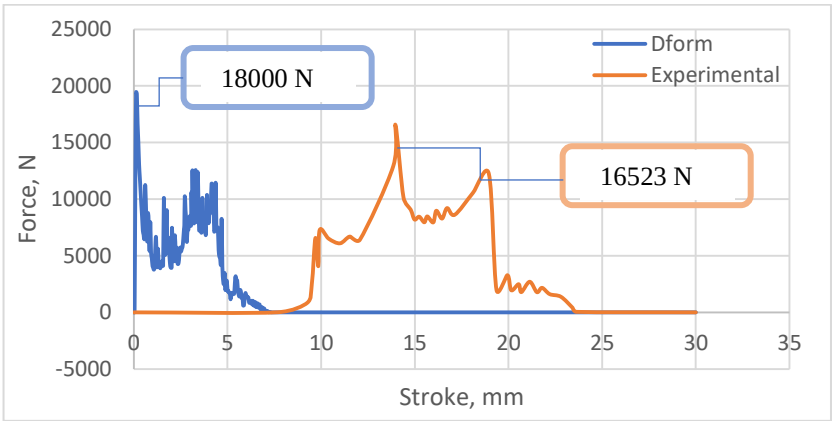

Figure 5.33. Comparison of the graphics obtained from the experimental and simulation punching process made with R2 punch.

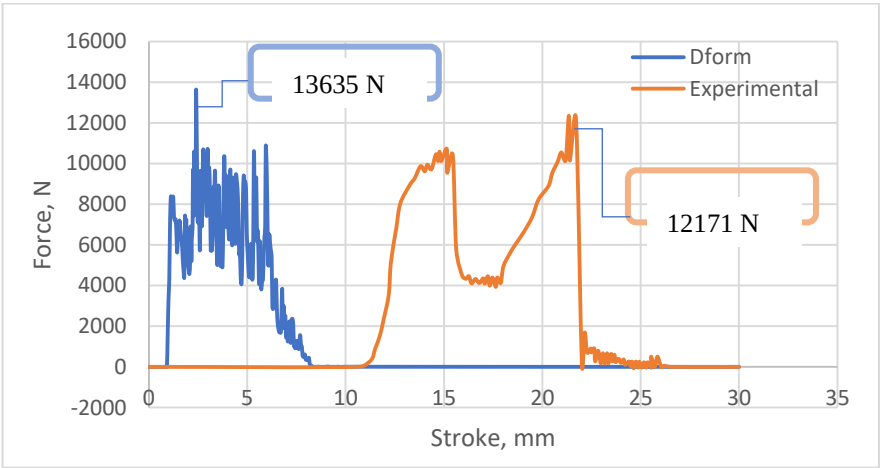

Figure 5.34. Comparison of the graphics obtained from the experimental and simulation punching process made with P16 punch.

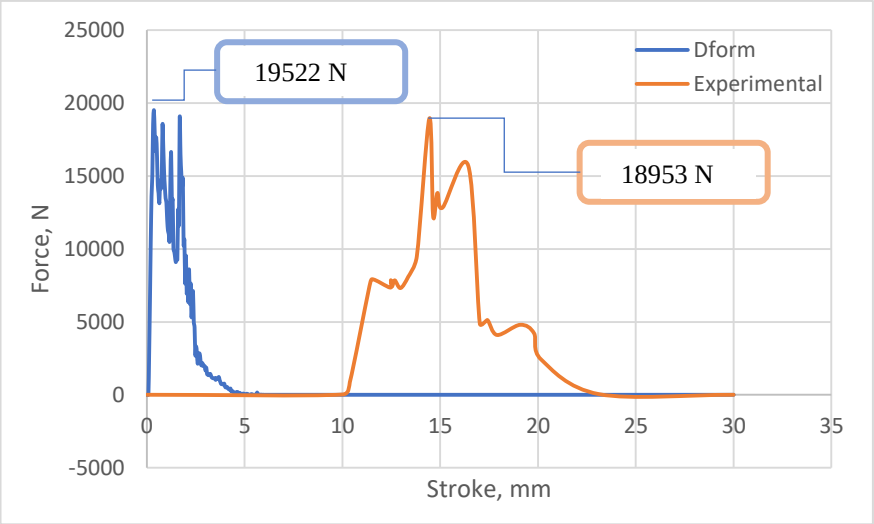

Figure 5.35. Comparison of the graphics obtained from the experimental and simulation punching process made with V16 punch.

There is a correlation between experimental and simulation studies, and the difference is thought to be due to the meshing density, the material model not truly modelled, or inability to model imperfections that exist in the material. As a result of simulation and experimental punching studies, lower punching forces were obtained from R1, R2, V16, P16 punches compared to flat punch. As explained in the previous pages, different punch geometries showed different punch force values due to differences in contact surfaces. As can be understood from two studies punch tip angle is very important because it affects the contact area, thereby it affects the punch force too. According to the experimental and numerical studies, the optimum cutting surface properties and punching forces obtained from P16 punch.

As can be understood from two studies punch tip angle is very important because it affects the contact area, thereby it affects the punch force too. Significant reduction in punching forces has been achieved with different punch geometries. Punch forces were reduced by 60% for the R1 punch, 65% for the V16 punch, 70% for the R2 punch, and 78% for the P16 punch. In similar studies in the literature, it has been stated that the force values decrease with the increase of the punch angle and also the clearance is quite effective on the force [69]. The consistency of the observed force values in experimental studies has been verified with finite element studies. Thus, instead of performing extra experimental studies for the precision, the results were obtained close

to experimental data under appropriate boundary conditions. In addition, in the experimental studies, it was ensured that there were no material-related defects and that the errors that could occur during the experiment. At the same time, the contact relationship between bevelled punches and the material could be understood more concretely by finite element analysis. Therefore, the finite element method can be considered to be extremely useful in manufacturing processes such as punching and piercing.

Another important issue for a part formed by punching is the cutting surface properties. The cutting surface properties are very effective on stretchability as explained in the previous [70]. In this case, it is explained in the previous that the most critical areas are the cutting surfaces. Especially on the cutting surface, the fracture area generally is desired as small as possible. Therefore, predictability of the cutting surface is very important for AHSS steels. It has been observed that the use of damage models is also very important to obtain results that are closest to real cutting surface properties. When using the Cockroft-Latham damage model in the studies, it was seen that the optimum damage coefficient for DP800 steel was 1.5 to predict similar cutting surface properties. Finally, close cutting surface properties were obtained by experimental studies. Using different damage models can lead to more realistic results. In this regard, [71] used SPCC materials to obtain the closest to real cutting surface in finite elements. They modelled it as finite elements with Marc Mentat and tried to determine the C damage constant using the Oyane and Cockroft-Latham damage model. As a result of his studies, he found the C value as 0.96 for the Oyane damage model and 1.5 for the Cockroft-Latham damage model. As a result, they found that the most accurate estimate for the onset of ductile fracture can be obtained using the Oyane damage model. [68] modified the Rice-Tracey criteria in order to accurately predict crack initiation by taking into account the formation of voids in shape and volume changes. [69] used the Cockroft-Latham damage model to examine the effects of clearance values between punch and die on fracture and shear regions. In the studies, they observed that there is a correlation between experimental and theoretical results. The using of damage criteria in studies on damage estimation is very important for damage estimation.

Different cutting surface properties have been obtained as a result of the operations with punches with different geometries. It has been observed that the fracture zone increases, and the amount of burr decreases especially with increasing inclination [67]. in their work with TRIP800 grade AHSS steel they observed that there was a decrease in the fracture zone as the clearance values increased. Therefore, different clearance values may be important for determining the minimum amount of fracture zone with bevelled punch. In addition, there is no uniform cutting surface in R1, R2 and V16 punches. For this reason, performing hole expansion tests on parts with non-uniform cutting surfaces can be very important in determining mechanical properties punched parts. Therefore, it is very important to make hole expansion tests on parts punched with punches with different geometries for more reliable designs.

In addition to all these, studies have shown that punches with different geometries affect the dimensional consistency of the holes. It is thought that this situation may be related to spring back characteristic of the material and the clearances. The closest dimensions to the nominal size 20 mm were obtained from the P16 punch. Dimensional consistency decreases from the P16 punch to the R2, V16, R1 and P0 punch, respectively. Therefore, the use of inclined punches can be recommended in situations where dimensional consistency is important.

PART 6

CONCLUSION

In this study, DP steel which has a very important place for the automotive industry, was used. In the studies, DP800 steel was punched with a punch with 5 different geometries and force values were obtained. In addition, DP800 material model was modeled and punching operations have been conducted with the commercial finite element software SIMUFACT and DEFORM. Cutting surface and stress distributions are analyzed with 2D simulations. Force graphs obtained from experimental and simulation studies have been compared with each other. Consequently, the following results have been accomplished:

- As a result of 2D simulation studies, the critical damage constant for DP800 sheet steel was determined. As a result, it has been observed that the shear zone where breaking starts is 28% of the thickness.
- It has been observed that the most uniform cutting surfaces are obtained from punching processes with flat and P16 punches Also, lowest punching forces obtained from P16 punch.
- As a result of the experimental and finite element analysis, it has been observed that punching forces decrease due to the cutting angle in punches with inclined surface.
- It has been observed that different punch geometries affect the stress distribution and fracture formation on the part. And understood that punch tip surface area affects the punch force.
- Experiments with the R1 and R2 punch have shown that increasing the cutting angle can reduce the punching forces because of contact area and force relation.

- In the punching experiments performed with the finite element method, it has been observed that the force values match the force values obtained from the experimental methods.
- As a result of punching experiments with 5 different geometries, it was observed that the highest punch force occurred in the experiments performed with flat punch, while the lowest punch forces occurred in the experiments with P16 punch.

REFERENCES

1. Hulka, K., "Modern multi-phase steels for the automotive industry", ***Trans Tech Publications Ltd,*** 4(14): 101-110 (2003).

2. Gilchrist, I., & Crossland, B., "The forming of sheet metal using underwater electrical discharges", ***In IEE Conference Publication***, 3(8): 92 (1967).

3. Johnson, W., "Piercing and hole-flanging of sheet metals: a survey", ***Poinconnage Et Formage De Collerettes Dans Les Toles Metalliques: Un Tour D'horizon,*** 77(4):585-606 (1980).

4. Pepelnjak, T., Kayhan, E., ve Kaftanoglu, B., "Analysis of non-isothermal warm deep drawing of dual-phase DP600 steel", ***International Journal of Material Forming***, 12(2): 223–240 (2019).

5. Pepelnjak, T., & Kaftanoglu, B., "Finite element analysis of non-isothermal warm deep drawing of dual phase steel", ***In MATEC Web of Conferences,*** 80(14): 3 (2016).

6. Wu, X., Bahmanpour, H., ve Schmid, K., "Characterization of mechanically sheared edges of dual phase steels", ***Journal of Materials Processing Technology***, 212(6): 1209–1224 (2012).

7. Bernert, W., Bzdok, M., Davis, J., Fekete, J., Fitzgerald, K., Noel, J. & Zuidema, B., "Advanced high-strength steel product and process applications guideline", ***Auto/steel partnership,*** USA, 12-20 (2008).

8. Buzzichelli, G. ve Anelli, E., "Present status and perspectives of European research in the field of advanced structural steels", ***ISIJ International***, 42 (12): 1354–1363 (2002).

9. Hausmann, K., Krizan, D., Spiradek-Hahn, K., Pichler, A., and Werner, E., 'The influence of Nb on transformation behavior and mechanical properties of TRIP-assisted bainitic–ferritic sheet steels', ***Materials Science and Engineering: A,*** 58(8): 142–150 (2013).

10. Cheung, C. F., Lee, W. B., ve Chiu, W. M., "An investigation of tool wear in the dam-bar cutting of integrated circuit packages", ***Wear***, 237(2): 274–282 (2000).

11. Park, N., Huh, H., Lim, S. J., Lou, Y., Kang, Y. S., ve Seo, M. H., "Fracture-based forming limit criteria for anisotropic materials in sheet metal forming", ***International Journal of Plasticity***, 9(6): 1–35 (2017).

12. Farías, D., de Kanter (Jens), Witteman, W. J., Geers, M. G. D., & Carless, S., "Bake Hardening Response of DP800 and the Influence on the'in Service Performance", ***Technische Universiteit Eindhoven,*** Eindhoven, Hollanda, 23-27 (2006).

13. Keeler, S. ve Kimchi, M., "Advanced high-strength steels application guidelines V5", ***WorldAutoSteel***, USA, 22-25 (2015).

14. Nesterova, E. V, Bouvier, S., ve Bacroix, B., "Microstructure evolution and mechanical behavior of a high strength dual-phase steel under monotonic loading", ***Materials Characterization***, 10(2): 152–162 (2015).

15. Azizi-Alizamini, H., Militzer, M., ve Poole, W. J., "Formation of ultrafine grained dual phase steels through rapid heating", ***ISIJ International***, 51(6): 958–964 (2011).

16. Tamarelli, C. M., "AHSS 101: the evolving use of advanced high-strength steels for automotive applications", ***Steel Market Development Institute***, 1(4): 42 (2011).

17. Yu, Z., Barabash, R., Barabash, O., Liu, W., ve Feng, Z., "Microscopic deformation in individual grains in an advanced high-strength steel", ***Jom***, 65(1): 21–28 (2013).

18. Unruh, G. C., "Understanding carbon lock-in", ***Energy Policy***, 28(12): 817–830 (2000).

19. Khan, M. I., Kuntz, M. L., ve Zhou, Y., "Effects of weld microstructure on static and impact performance of resistance spot welded joints in advanced high strength steels", ***Science and Technology of Welding and Joining***, 13(3): 294–304 (2008).

20. Tumuluru, M., "The effect of coatings on the resistance spot welding behavior of 780 MPa dual-phase steel", ***Welding Journal,*** 86(6): 161 (2007).

21. Pouranvari, M. ve Marashi, S. P. H., "Critical review of automotive steels spot welding: Process, structure and properties", ***Science and Technology of Welding and Joining***, 18(5): 361–403 (2013).

22. Irie, T., Satoh, S., Hashiguchi, K., Takahashi, I., Ve Hashimoto, O., "Metallurgical factors affecting the formability of cold-rolled high strength steel sheets", ***Transactions of the Iron and Steel Institute of Japan***, 21(11): 793–801 (1981).

23. Furukawa, T., Morikawa, H., Endo, M. Takechi, Koyama, H. K. O., "Process Factors for Cold-rolled Dual-phase Sheet Steels," Transactions of the Iron and Steel Institute Of Japan", ***Transactions of the Iron and Steel Institute of Japan***, 21(11): 812–819 (1981).

24. Kankanamge, N. D. ve Mahendran, M., "Mechanical properties of cold-formed steels at elevated temperatures", ***Thin-Walled Structures***, 49(1): 26–44 (2011).

25. Al-Abbasi, F. M. ve Nemes, J. A., "Micromechanical modeling of dual phase steels", ***International Journal of Mechanical Sciences***, 45(9): 1449–1465 (2003).

26. Granbom, Y., "Structure and mechanical properties of dual phase steels: An experimental and theoretical analysis", ***School of Industrial Engineering and Management (ITM), Materials Science and Engineering, Mechanical Metallurgy,*** Stockholm, Sweden, 21-32 (2010)

27. Rana, R. ve Singh, S. B., "Automotive steels: design, metallurgy, processing and applications", ***Woodhead Publishing***, Berlin, Germany, 12-22 (2016).

28. Kumar, A., Singh, S. B., ve Ray, K. K., "Influence of bainite/martensite-content on the tensile properties of low carbon dual-phase steels", ***Materials Science And Engineering: A***, 474(2): 270–282 (2008).

29. Saeidi, N. ve Ekrami, A., "Comparison of mechanical properties of martensite/ferrite and bainite/ferrite dual phase 4340 steels", ***Materials Science and Engineering: A***, 523(2): 125–129 (2009).

30. Ramazani, A., Pinard, P. T., Richter, S., Schwedt, A., ve Prahl, U., "Characterisation of microstructure and modelling of flow behaviour of Characterisation of microstructure and modelling of flow behaviour of bainite-aided dual-phase steel", ***Computational Materials Science***, 3(3): 23-35 (2014).

31. Park, K., Nishiyama, M., Nakada, N., Tsuchiyama, T., & Takaki, S., "Effect of the martensite distribution on the strain hardening and ductile fracture behaviors in dual-phase steel", ***Materials Science And Engineering: A***, 60(4): 135–141 (2014).

32. Peng-Heng, C. ve Preban, A. G., "The effect of ferrite grain size and martensite volume fraction on the tensile properties of dual phase steel", ***Acta Metallurgica***, 33(5): 897–903 (1985).

33. Jiang, Z., Guan, Z., ve Lian, J., "Effects of microstructural variables on the deformation behaviour of dual-phase steel", ***Materials Science and Engineering: A***, 190(2): 55–64 (1995).

34. Calcagnotto, M., Adachi, Y., Ponge, D., ve Raabe, D., "Deformation and fracture mechanisms in fine- and ultrafine-grained ferrite/martensite dual-phase steels and the effect of aging", ***Acta Materialia***, 59(2): 658–670 (2011).

35. Alzahougi, A. R. O., "Investigation and simulation of resistance spot welding using dp600 steel in automotive industry", ***Phd. Thesis. Kabauk University,*** Karabuk, Turkey, 45-51 (2020).

36. Tisza, M., "Development of Lightweight Steels for Automotive Applications", ***Engineering Steels and High Entropy-Alloys, IntechOpen***, Berlin, Germany, 33-36 (2020).

37. Waterschoot, T., Kestens, L., ve De Cooman, B. C., "Hot rolling texture development in CMnCrSi dual-phase steels", ***Metallurgical and Materials Transactions A***, 33(4): 1091 (2002).

38. Amirthalingam, M., "Microstructural Development during Welding of TRIP Steels", ***Mechanical, Maritime and Materials Engineering, Faculty of 3mE, Delft University of Technology,*** Delft, Netherlands, 171 (2010).

39. Oliver, C., "Dual Phase Steel Characterization for Tube Bending and Hydroforming Applications", ***University of Windsor,*** Canada, 34-41 (2010).

40. Kuang, S., Kang, Y., Yu, H., ve Liu, R., "Simulation of intercritical austenization of a C-Mn cold rolled dual phase steel", ***Materials Science Forum***, 57(8): 1062–1069 (2008).

41. Güral, A., Bostan, B., ve Özdemir, A. T., "Heat treatment in two phase region and its effect on microstructure and mechanical strength after welding of a low carbon steel", ***Materials & Design***, 28(3): 897–903 (2007).

42. Vural, M. ve Akkus, A., "On the resistance spot weldability of galvanized interstitial free steel sheets with austenitic stainless steel sheets", ***Journal of Materials Processing Technology***, 15(3): 1–6 (2004).

43. Sodjit, S. ve Uthaisangsuk, V., "Microstructure based prediction of strain hardening behavior of dual phase steels", ***Materials & Design***, 4(1): 370–379 (2012).

44. Sun, D. Q., Lang, B., Sun, D. X., ve Li, J. B., "Microstructures and mechanical properties of resistance spot welded magnesium alloy joints", ***Materials Science and Engineering: A***, 4(60): 494–498 (2007).

45. Sarwar, M. ve Priestner, R., "Influence of ferrite-martensite microstructural morphology on tensile properties of dual-phase steel", ***Journal of Materials Science***, 31(8): 2091–2095 (1996).

46. Loisy, C. ve Cerepi, A., "Radon-222 as a tracer of water–air dynamics in the unsaturated zone of a geological carbonate formation: Example of an underground quarry", ***Chemical Geology***, 29(6): 39–49 (2012).

47. Matlock, D. K., Speer, J. G., ve De Moor, E., "Recent AHSS developments for automotive applications: processing, microstructures, and properties", ***Proceedings of the Addressing Key Technology Gaps in Implementing Advanced High-Strength Steels for Automotive Lightweighting, USCAR Offices,*** Southfield, USA, 9–10 (2012).

48. Kahraman, N., "The influence of welding parameters on the joint strength of resistance spot-welded titanium sheets", ***Materials & Design***, 28(2): 420–427 (2007).

49. McCallum, B., "Characterization of DP600 Steel Subject to Electrohydraulic Forming", ***University of Windsor,*** Canada, 56-61 (2014).

50. Lim, Y., Ulsoy, A. G., ve Venugopal, R., "Process control for sheet-metal stamping", ***Springer***, New York, 12-18 (2013).

51. Maiti, S. K., Ambekar, A. A., Singh, U. P., Date, P. P., ve Narasimhan, K., "Assessment of influence of some process parameters on sheet metal blanking", ***Journal of Materials Processing Technology***, 102(3): 249–256 (2000).

52. Samuel, M., "FEM simulations and experimental analysis of parameters of influence in the blanking process", ***Journal of Materials Processing Technology***, 84(3): 97–106 (1998).

53. Johansonn, B. ve Olsson, K., "Tooling solutions for advanced high strength steels", **In *Uddeholm Automotive Tooling Seminar,*** 4(7): 777-780 (2005).

54. Shih, H.-C. ve Chiriac, C., "The Effects of AHSS Shear Edge Conditions on Edge Fracture", ***In International Manufacturing Science and Engineering Conference***, 49(46): 599-608 (2010).

55. Wai Myint, P., Hagihara, S., Tanaka, T., Taketomi, S., ve Tadano, Y., "Application of Finite Element Method to Analyze the Influences of Process Parameters on the Cut Surface in Fine Blanking Processes by Using Clearance-Dependent Critical Fracture Criteria", ***Journal of Manufacturing and Materials Processing***, 2(2): 26 (2018).

56. MacKensen, A., Golle, M., Golle, R., ve Hoffmann, H., "Experimental investigation of the cutting force reduction during the blanking operation of AHSS sheet materials", ***CIRP Annals - Manufacturing Technology***, 59(1): 283–286 (2010).

57. Hambli, R., "Prediction of burr height formation in blanking processes using neural network", ***International Journal of Mechanical Sciences***, 44(10): 2089–2102 (2002).

58. Chiriac, C. ve Shih, H.-C., "Investigations on Sheared Edge Damage of Dual Phase 780 Steel", ***Materials Science and Technology conference***, Ohio, USA, 617–626 (2011).

59. Behrens, B., Bouguecha, A., Vucetic, M., Krimm, R., Hasselbusch, T., ve Bonk, C., "Numerical and experimental determination of cut-edge after blanking of thin steel sheet of DP1000 within use of stress based damage model", ***Procedia Engineering,*** 81(3): 1096–1101 (2014).

60. Hambli, R. ve Reszka, M., "Fracture criteria identification using an inverse technique method and blanking experiment", ***International Journal of Mechanical Sciences***, 44(7): 1349–1361 (2002).

61. Altan, T. ve Tekkaya, E., "Sheet metal forming: Processes and Applications", ***ASM International,*** Ohio, USA, 1–15 (2012).

62. Pu, C., Zhou, D., Makrygiannis, P., Wu, W., Jia, Y., Zhu, F., Du, C., ve Wang, Y. W., "A Comprehensive Study of Hole Punching Force for AHSS", ***SAE Technical Papers***, 2(8): 1–9 (2018).

63. Mori, K. I., "Review of shearing processes of high strength steel sheets", ***Journal of Manufacturing And Materials Processing***, 4(2): 54 (2020).

64. Gu, J., Kim, H., Shih, H. C., ve Dykeman, J., "Effects of Blanking Conditions to Edge Cracking in Stamping of Advanced-High Strength Steels (AHSS)", ***SAE Technical Papers***, 3(4): 1–8 (2018).

65. Levy, B. S. ve Van Tyne, C. J., "Review of the shearing process for sheet steels and its effect on sheared-edge stretching", ***Journal of Materials Engineering and Performance***, 21(7): 1205–1213 (2012).

66. Ghosh, M., Kumar, K., and Mishra, R. S., "Friction stir lap welded advanced high strength steels: Microstructure and mechanical properties", ***Materials Science and Engineering: A,*** 528 (28): 8111–8119 (2011).

67. Gu, J., Kim, H., Shih, H. C., & Dykeman, J. "Effects of blanking conditions to edge cracking in stamping of advanced-high strength steels", ***SAE Technical Paper,*** 20(18): 626 (2018).

68. Kwak, T. S., Kim, Y. J., & Bae, W. B., "Finite element analysis on the effect of die clearance on shear planes in fine blanking", ***Journal of Materials Processing Technology,*** 130(1): 462-468 (2002).

69. Zhao, Z., Zhuang, X. C., & Xie, X. L., "An improved ductile fracture criterion for fine-blanking process", ***Journal of Shanghai Jiaotong University (Science),*** 13(6): 702-706 (2008).

70. Kim, H., Shang, J., Dykeman, J., Samant, A., & Hoschouer, C., "Practical evaluation and prediction of edge cracking in forming advanced high strength steels (AHSS)", ***SAE Technical Paper.*** 20(17): -300-308 (2017).

71. Shih, H. C., Hsiung, C. K., & Wendt, B., "Optimal production trimming process for AHSS sheared edge stretchability improvement", ***SAE Technical Paper,*** 20(14): 223-240 (2014).

RESUME

Abdul Salam SAIER was born in Braak in 1990 and he graduated first, elementary and high school in this city, after that, he started an undergraduate program in Higher Institute for Comprehensive Professions Department Mechanical engineering in 2008. Then in 2018, He started in Karabük University, Technology Faculty, Department of Manufacturing Engineering. M. Sc. education.

CONTACT INFORMATION

Address : Karabük University
Graduate School of Natural & Applied Science
Demir-Çelik Campus/KARABUK
E-mail : abdulsalamsaier@gmail.com